

# Graphitic Carbon Films Across Systems

Emily E. Hoffman<sup>1</sup> · Laurence D. Marks<sup>1</sup>

Received: 8 June 2016 / Accepted: 14 July 2016  
© Springer Science+Business Media New York 2016

**Abstract** When metal surfaces come into contact, lubricants are used to overcome friction. Various forms of hydrocarbons play a central role in lubrication, through both liquid lubricants and surface coatings. Solid lubricants like graphite and complex surface coatings such as diamond-like carbon have led to great advancements in friction mitigation. In addition to these designed carbon films, unintentional carbon films can also spontaneously form during metal–metal sliding. Here, we analyze various systems that produce carbon films, focusing on systems with cyclical metal sliding, hydrocarbon lubricants, and catalytic activity. The systems we analyze include friction polymers, diamond-like carbon coatings, varnish from industrial machines, metal-on-metal hip implants, microelectromechanical systems, and catalysis coke. These films, analyzed at the nanoscale, are primarily graphitic carbon with local regions of  $sp^2$  bonding. The graphitic carbon can act as a lubricant in some systems and not in others. Through comparing these various fields, we seek to better understand the formation, evolution, and friction properties of carbon films. Through design and control of carbon films formation, we can control triboactivity to improve system performance.

**Keywords** Solid lubricants · Solid lubrication mechanisms · Carbon · Graphite · Lubricant degradation

---

✉ Emily E. Hoffman  
emilyhoffman2016@u.northwestern.edu

Laurence D. Marks  
L-marks@northwestern.edu

<sup>1</sup> Department of Materials Science and Engineering,  
Northwestern University, Evanston, IL 60208, USA

## 1 Introduction

In research, forming deep connections to make significant progress is difficult. As science becomes more complex, fields specialize and concentrations deepen. Often large advancements require connections across fields: collaboration is necessary for innovative discoveries. Here, we present a review that attempts to connect various fields that study graphitic films. We show commonalities between thin carbon films in seemingly diverse areas to demonstrate how the similarities between these fields of research can be utilized for practical advancements in lubrication.

When two surfaces come into sliding contact, the tribology is key to performance. The primary goal of tribology research is mitigating friction and finding beneficial lubrication methods. Understanding friction drives design of systems across size scales, from industrial motors to precise micron-scale gears, shown in Fig. 1 [1, 2]. Surface coatings, liquid lubricants, and solid lubricants are all relevant to tribology.

In lubrication methods, hydrocarbons play a central role. Hydrocarbons are used in standard industrial lubricating oils, are deposited as lubricious carbon films, and can be unintentionally incorporated into systems from the air. Carbon that unintentionally enters the system can spontaneously form deposits that become a film, similar to designed deposited films. Carbon in the system or from the environment reacts from heat, catalysis, friction, and cycling to continuously evolve to a final carbon film. This film is usually thin, slick, and described as a high molecular weight polymer. It is often graphitic, i.e., it contains some fraction of  $sp^2$  carbon–carbon double bonds and not just single  $sp^3$  bonds. In general, these are local  $sp^2$  bonds, or perhaps small nanoscale regions of continuous aromatic bonding, not a full continuous network of graphite sheets.

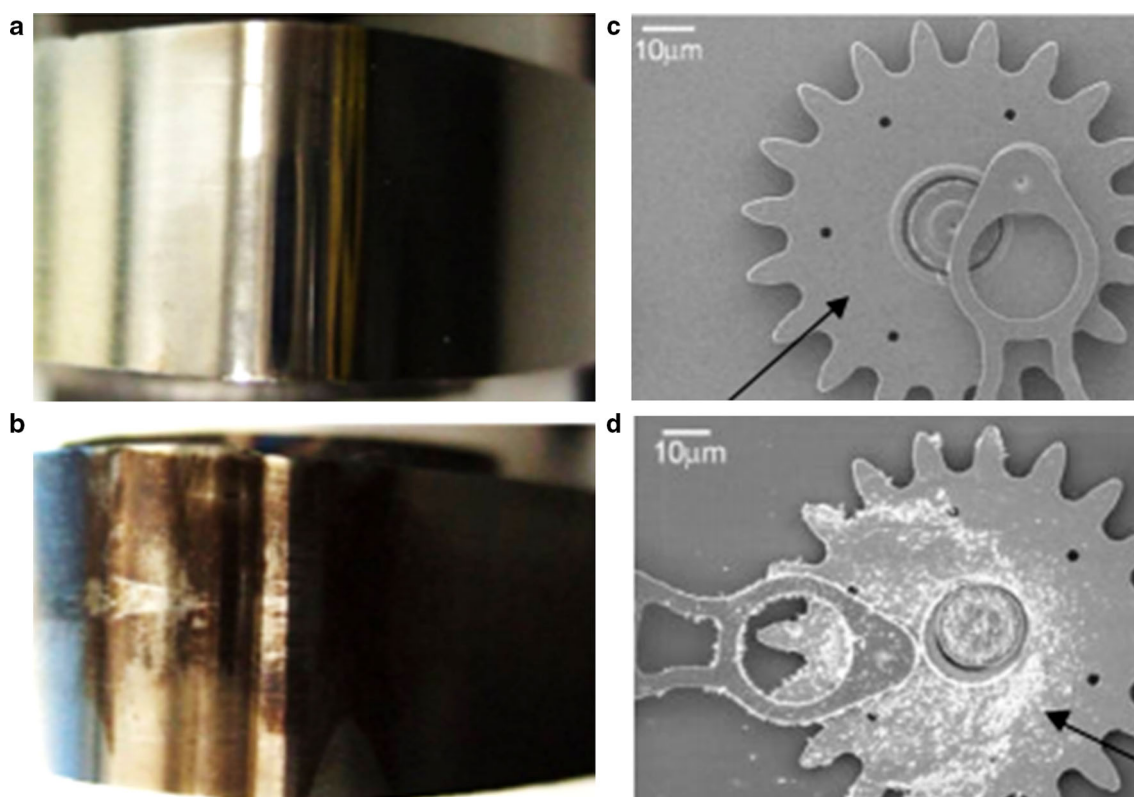


**Fig. 1** Wear tests using PAG oil formulations, forming **a** minimal wear and **b** varnish film formation [1]. At a different size scale, MEMS gears **c** before testing and **d** after failure caused by adhesion [2]

This film is present in different systems by different names, yet on the nanoscale, it is the same thin layer of partially graphitic carbon. This concept is illustrated in Fig. 2.

To explain the connections between these fields, this review will introduce systems of interest, explain mechanisms of film formation, and conclude with a discussion of opportunities. The systems included for analysis are major fields of tribology and carbon film research, where there are both recent and decades of older data to consider. The fields included are friction polymers, diamond-like carbon (DLC) coatings, varnish from industrial lubricants, the tribolayer from metal-on-metal (MoM) hip replacements, microelectromechanical systems (MEMS), and catalysis coke. In these systems, all the films, except for coke, are considered tribolayers, layers that form during frictional contact. Tribolayers or tribofilms form due to triboactivity or tribochemical reactions. In catalysis, there is no friction, so this system serves as a comparison as there are chemical reactions without triboactivity. Because coke is an included system, we refer to the graphitic carbon products as carbon *films* as opposed to carbon *tribolayers* when addressing all systems collectively.

The motivation for a combined study comes from the opportunity for mutually beneficial research. Hsu and Gates [3] discussed that our understanding of the nature of

tribochemistry is limited, partly because it is largely empirical. The need for future understanding is crucial because as new materials emerge, use is often blocked by lack of knowledge of how the materials can be effectively lubricated. Ineffective lubrication can result in premature failure or product recall. In the presented systems, the carbon films affect performance differently: some are protective and some damaging. Even though they are all partially graphitic carbon films, the questions at hand are: what causes the differences and can the beneficial systems be exploited for better design across systems?

This review is organized into three sections: systems, mechanisms of formation, and discussion. The first section provides a general overview of the six primary systems: friction polymers, DLC coatings, varnish, hip implant tribolayers, MEMS, and coke. These represent general fields of research, each with a wide breadth of tribolayer research; we provide a brief summary and context for each. Finally, we give three specific examples of carbon tribolayers that are relevant for discussion. These systems and examples are not an exhaustive collection; we predict that more parallel systems could be compared from even broader fields.

The second section is on the mechanisms of formation of carbon films. This section describes processes and

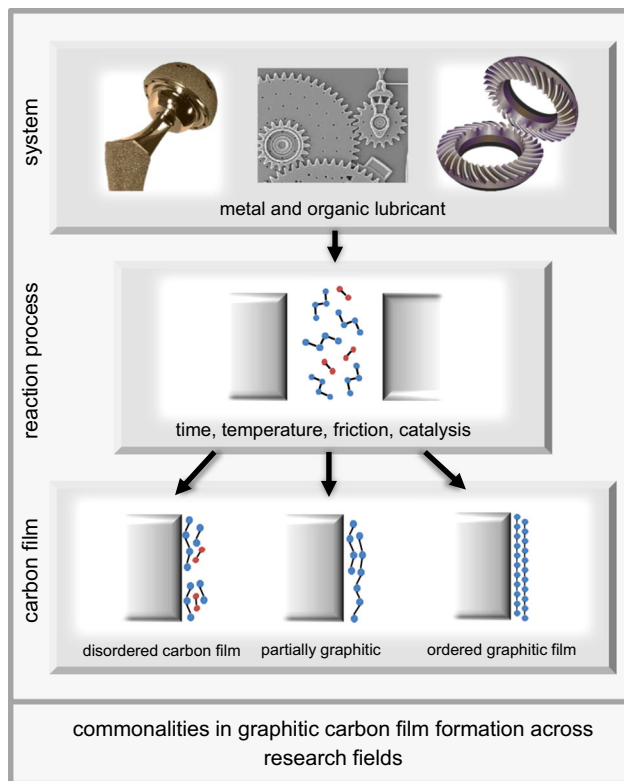


**Fig. 2** Metal-on-metal hip implants, MEMS gears, and industrial machines are all lubricated with hydrocarbons. Through friction and wear at the metal interface, the organic material reacts to form similar carbon films

reactions that occur to convert organic precursors into graphitic carbon films. The mechanisms covered include pressure, temperature, and friction; deposition and absorption; polymerization and organometallics; catalytic activity; graphitization; and particle interaction. The mechanisms are often common across systems, and so, they are grouped as mechanisms and not as systems.

The third and final section is the discussion section. We summarize the key similarities between the systems and mechanisms, highlighting the main trends. To link the different systems, we present a general thermodynamic argument for carbon developing into graphitic bonding. Lastly, the future opportunities between these fields are emphasized. The possible connections in research methods and analysis techniques show promise to significantly advance each field.

## 2 Systems

This section presents an introduction to the six primary systems: friction polymers, DLC coatings, varnish, hip implant tribolayers, MEMS, and coke. All of these films are primarily carbon and have a significant portion of

graphitic bonding. The systems are all triboactive, except for coke, which is catalytically and thermally active.

### 2.1 Friction Polymers

The name “friction polymer” is the most widely used term to describe carbonaceous deposits on triboactive surfaces. Narrower fields focus on specific tribofilms and give them more particular names, which we will explore in later sections. Friction polymer is also one of the oldest terms, with common use in research as far back as the 1950 s [4]. Friction polymer systems tend to be metal-on-metal, such as electrical relay switches, gears, engines, and other machines with rolling, sliding, or rubbing contacts. Friction polymers include tribofilms that are classified as both helpful and harmful to performance, depending on the study. What makes a beneficial friction polymer is not always well understood.

In friction polymers, there are common descriptors that appear across studies. The appearance of a friction polymer is brown and slick, usually with a reddish hue. The friction polymer film has a buildup that can be wiped away and a thin, stubbornly adhered layer beneath, shown in Fig. 3a [5]. The polymer sometimes improves friction, yet the beneficial properties can change through small alterations of temperature, pressure, number of cycles, or carbon concentration [4, 6]. The substrates that create friction polymers are usually oxide-forming metals, such as palladium, chromium, molybdenum, or iron, although usually just one surface needs to be metal [4, 7–9]. The film’s carbon source can be standard lubricating oils or carbonaceous vapors, which replicate situations where the carbon source is from the atmosphere [10, 11]. Often friction polymer work calls the carbon deposits amorphous, yet they also include descriptions that point to signs of graphitic carbon. Many studies note evidence of reduced wear and Raman spectra, showing graphitic bonding, such as in Fig. 4a [12, 13]. To understand the tribochemical reactions that can lead to partially graphitic carbon, studies have characterized the organometallic species, insoluble products, and the molecular weight [14–16]. The mechanisms of these reactions will be discussed in the next section to show the common mechanisms across the carbon film systems.

The direction of friction polymer research was well summarized in the 2006 review article by Hsu et al. [3]. They described the need to further understand the formation of these lubricating films because much of the information is empirical and limited to the steel–hydrocarbon system. The metals–hydrocarbons research suggests that thermochemistry and organometallics dominate the chemical reactions, whereas in semiconductors, electrostatic charge and electron emission is important for

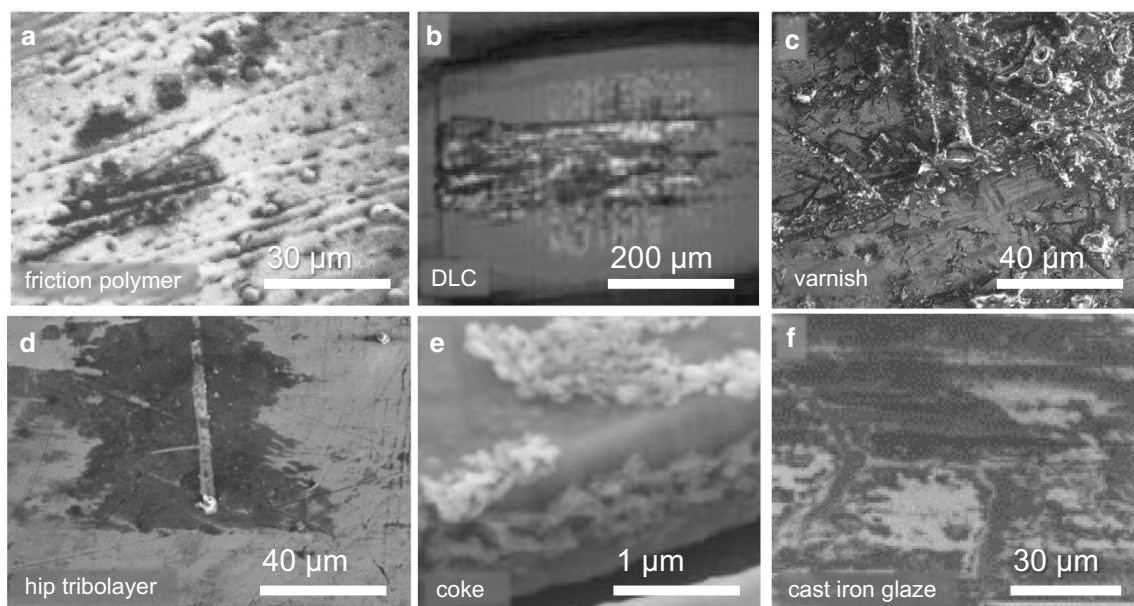


**Fig. 3** Similar micron-scale appearance of the carbon films after sliding contact. **a** Friction polymer [5], **b** DLC [20], **c** varnish tribolayer, **d** hip explant tribolayer [57], **e** MEMS wear film [2], and **f** cast iron glaze [106]

tribochemistry [16, 17]. Through understanding reactivity and mechanisms, the various factors that create friction polymers can be understood, such as how organometallic chemistry is central to forming high molecular weight reaction products that lead to effective lubrication [16]. By understanding how the bond breakage and bond formation occurs in various systems, friction polymers can be predicted and controlled for effective lubrication. To emphasize the pending questions of the field, Hsu et al. asks “What constitutes an effective film? Under what conditions (i.e., reactions and starting materials) will an effective film be formed? Under what conditions will the film not form? What are the effects of nascent surfaces? Can we determine the kinetic rates of film formation?” [3]. Further nanoscale characterization of friction polymers could indicate how graphitic bonding and solid lubrication affects performance. In the following section, we continue to discuss films similar to friction polymers, and by connecting these fields, provide answers to some of these questions.

## 2.2 DLC Coatings

A commonly studied and well-known system of a carbon lubricant film is diamond-like carbon (DLC). Carbon films have been studied as early as the 1950s [18], with comprehensive studies on DLC by Eisenberg and Chabot in the 1970s [19]. They showed that the carbon film had nearest neighbor distances similar to diamond, was highly insulating, and was transparent, among other electrical and structural similarities to diamond. As DLC films have been

a popular research area, many functional varieties of the film and a breadth of applications have been explored. The breadth and depth of the DLC work can be used to help to explain the properties of other carbon films, across disciplines, designs, and phenomena.

DLC films are primarily made of carbon atoms that are extracted or derived from carbon-containing sources, such as solid carbon targets and liquid and gaseous forms of hydrocarbon and fullerenes. A DLC film after a sliding test is shown in Fig. 3b [20]. The modern multifunctional nanocomposite DLC films are now routinely produced by both chemical vapor depositions (CVD) and physical vapor deposition (PVD) [21]. The films can be designed to be extremely hard ( $\sim 90$  GPa) and resilient, while proving some of the lowest known friction coefficients [21]. A recent study showed an uncoated bearing failed after 32 million cycles, while a bearing with a one-sided DLC coating lasted 100 million cycles [22]. Applications including razor blades, microelectromechanical systems, engine parts, articulated hip joints, and machine tools have shown beneficial performance [23–26].

In a 2006 DLC review [21], Erdemir et al. discussed how the benefits of DLC come from the unique tribological properties, especially the transformation into a graphitic solid lubricant. It has been observed that  $sp^3$ -bonded carbon atoms in DLC film experience transition into  $sp^2$ -bonding [21], as shown in the Raman spectra in Fig. 4b [27] and EELS spectra in Fig. 5a [28]. Pastewka et al. [29] performed MD simulation and suggested that  $sp^3$  carbon bonds in diamond undergo a  $sp^3$ -to- $sp^2$  order–disorder



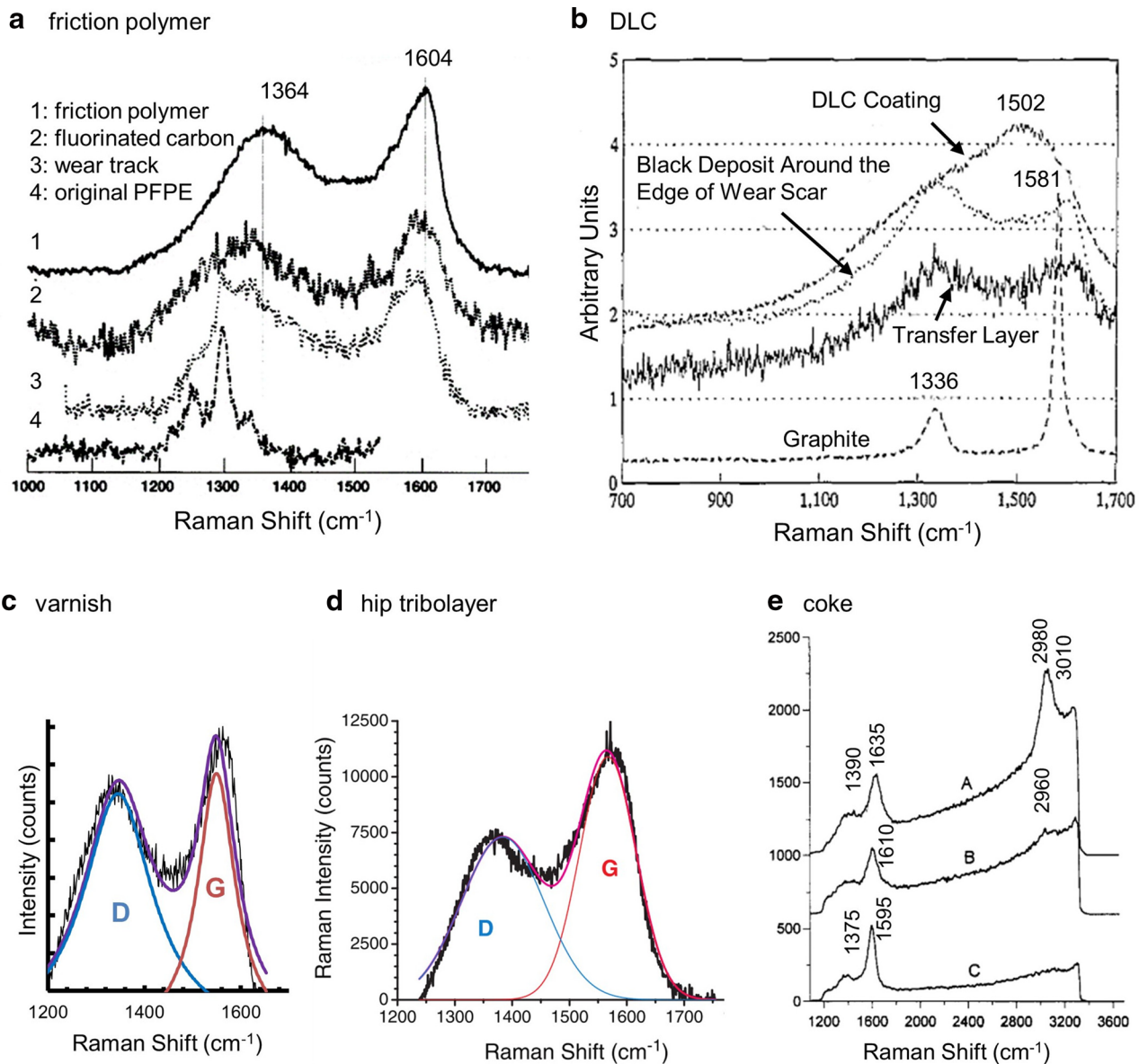


**Fig. 4** Raman spectra of **a** friction polymer [12], **b** DLC [27], **c** varnish, **d** hip explant tribolayer [57], and **e** catalyst [88]. All examples show a broad G band at  $\sim 1550\text{ cm}^{-1}$  and a D band at  $1350\text{ cm}^{-1}$ , indicating the presence of nanographitic carbon

transition upon polishing. The frictional behavior can be controlled through the chemical, physical, and mechanical interaction and physical roughness of the surface. The good adhesion of DLC films allows for high shear forces during sliding contact, while the friction values can range from 0.001 to 0.7 [22, 30].

In the context of this review, DLC films are critical to include as DLC research demonstrates key aspects of the graphitization process [31, 32]. We can use known phenomena of how DLC films are deposited, characterized, wear tested, and modified to extrapolate to other more uncontrolled or unknown systems. As discussed by Erdemir et al. [21], other forms of carbon including graphite,

graphite fluoride, carbon-carbon composites, and glassy carbon are also valuable as low-friction, solid lubricant engineering materials [22, 33–36].

### 2.3 Varnish in Industrial Machines

Varnish is found in industrial machinery. It is a carbon film that forms on metal surfaces when lubrication oil degrades. It is generally considered to be bad for applications, and much of varnish study is on how to remove it and prevent its formation. Information about varnish primarily comes from trade publications. These industrial articles are mostly written by companies that specialize in varnish filtration

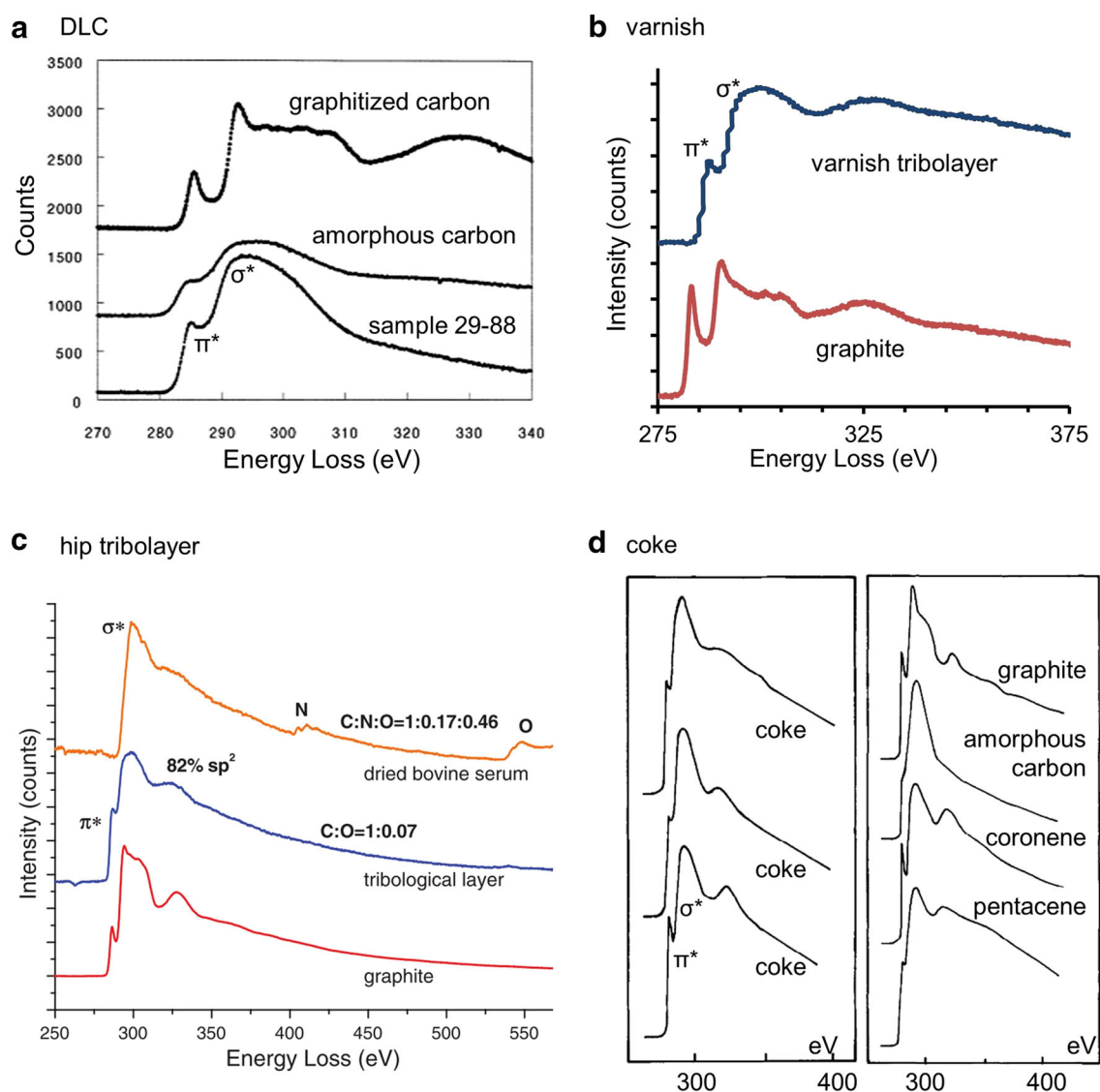


**Fig. 5** Electron energy loss spectroscopy of **a** DLC (*sample 29–88 in figure*) [28], **b** varnish, **c** hip explant tribolayer [57], and **d** catalyst substrate [92]. The ratio of the  $\pi^*$  peak to the  $\sigma^*$  peak indicates percent graphitic bonding [55, 56]. All spectra include graphite for reference

systems or varnish removal. Few industrial research studies focus on the composition of varnish once it has formed. We address varnish in two parts: the first part presents varnish as it is currently known in the field and the second part presents new nanoscale characterization studies on varnish. This original varnish research allows for more fruitful discussion later in the mechanisms and opportunities sections.

### 2.3.1 Varnish Literature

Modern hydraulic machinery uses oil to reduce friction for improved operation, and when the lubrication fails, a carbon film called varnish forms in the machinery that drastically reduces performance. Varnish is different

from the other films discussed because it is always considered damaging. Once lubricating oil begins to break down, the oil's contaminants form insoluble particles that deposit as a varnish film on moving parts [37–41]. The varnish film is an inhomogeneous, sticky brown residue that crusts to the surface of metal parts. It can have a cured, shiny appearance. Similar to other tribological films, two types of varnish are described. There are soft sludgy particles that stay in solution and can be removed with a filter, or on triboactive surfaces, there are thin, hard deposits that are difficult to remove, Fig. 6a, b, respectively [42]. Varnish films play a role in friction and wear, but varnish can be extremely varied, so it has been typically characterized by appearance and not by chemistry [39].

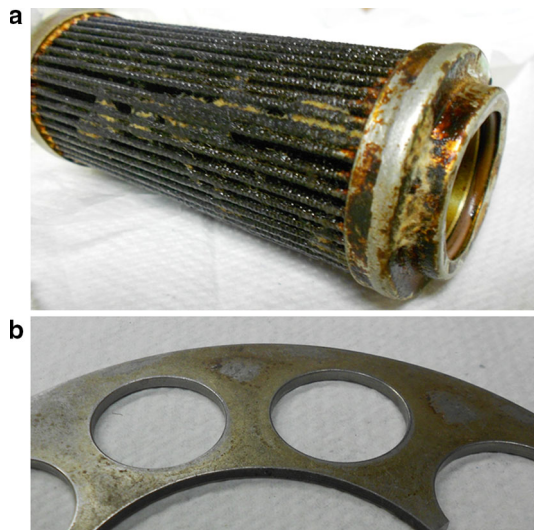


**Fig. 6** Two forms of varnish deposition: **a** show moving sludge varnish removed by a filter (part courtesy CC Jenson) and **b** deposited and cured shiny varnish film (part courtesy Dyna Power Parts)

Varnish, considered a “stubborn film,” is a constant battle in machinery lubrication, with varnish causing 85 % of hydraulic system failures [43]. Varnish causes sticking of moving mechanical parts, increase in component wear, and loss of heat transfer effectiveness [42, 44, 45]. Varnish is the product of the thermal/oxidative breakdown of hydrocarbons within oil which leads to a new chemistry of macromolecules [40–47]. This failure mode has become especially relevant as new developments in anti-oxidizing oils lead to oils that fail suddenly, without the slow and predictable degradation of previous oil formulas [39, 42, 48]. A majority of varnish literature comes from trade publications [40, 43, 44], where industrial leaders discuss the prevention and cleaning of varnish. Companies like ExxonMobil produce patents on varnish prevention systems [49, 50]. There is also a large amount of information on how to measure the chemical composition of oil and how to strain sludge particle from oil [44]. Additionally, the size of the degraded particles has become an area of interest. Previously, the method was to simply look at the oil to see whether it changed from a yellow to a reddish color; if it was reddish, it likely had varnish precursor particles. New techniques and ASTM standards [51] are recognizing submicron macromolecules formation and the presence of nanoparticles [42]. The composition of varnish is rarely mentioned, as the early development for prevention and the cleaning methods are considered more apt.

### 2.3.2 Original Varnish Research

We performed original research to investigate the presence of graphitic carbon in varnish. This level of nanoscale

characterization of the varnish film is not available in the literature.

A steel component with varnish buildup was acquired from Dynapower Parts. A SEM image of the thin area of varnish is shown in Fig. 3c. The part was a component of the Dynapower axial piston pump that run lubricants varying from 32 to 68 weight hydraulic oils to Dextron III. A thin and uniform area of varnish was measured with Raman spectroscopy using an Acton TriVista CRS Confocal Raman system with excitation radiation from an Ar–Kr 514.4 nm gas laser at  $\sim 10$  mW. As shown in Fig. 4c, a broad G band was present at  $1550\text{ cm}^{-1}$ , which showed the stretch vibration of  $\text{sp}^2$  bonding, and a D band was present at  $1350\text{ cm}^{-1}$ , which showed the breathing vibration in disordered  $\text{sp}^2$  carbon [52]. In the Raman spectra, the G-line position and broad D-line indicated that the film was composed of regions of nanographitic carbon [52]. The fraction of graphitic regions was determined from the intensity of the D peak relative to the intensity of G peak to be  $>80\%$  based on the standard analytical methods for carbons, e.g., [53, 54]. For the electron microscopy analysis, two different thin films were transferred to an Omniprobe transmission electron microscopy (TEM) grid. Approximately four different areas on two varnish tribolayer TEM samples were analyzed using a Gatan Imaging Filtering in a JEOL 2100F at 200 kV. Electron energy loss spectra (EELS) were calibrated using highly ordered pyrolytic graphite (HOPG). The varnish sample prepared was sufficiently thin, approximately 50 nm, to measure a carbon peak in EELS, as shown in Fig. 5b. The varnish  $\pi^*$  peak at 289 eV is characteristic of  $\text{sp}^2$  bonding, while the  $\sigma^*$  at 299 eV is characteristic of amorphous  $\text{sp}^3$  bonding, and the varnish peaks can be compared to the  $\pi^*$  peak found in the HOPG. The ratios of the varnish peaks show that the amount of graphitic carbon is approximately 80 % [55, 56]. Even though varnish has signatures of graphitic carbon, the varnish tribolayer formation is not within the design tolerances of the performance of hydraulic machine lubricating oils. The varnish causes damage to the machines and requires removal. Studying varnish, however, may allow for a controlled and beneficial film to form out of lubricating solutions. By understanding similar yet beneficial carbon films, such as DLC and MEMS coatings, improvements could be designed to reduce the negative impacts of varnish.

### 2.4 MoM Hips

Metal-on-metal (MoM) total hip replacements develop tribolayers after implantation in the human body, making this another informative system to study. Total hip replacements are made of two articulating components, the ball and cup, which can be made out of CoCrMo alloys,

ultra-high molecular weight polyethylene (UHMWPE), or alumina. The MoM tribofilm has been primarily studied on the metal-on-metal interface after *in vivo* studies and has been shown to be graphitic [57].

Early studies of the hip tribolayers considered the deposits to be of peripheral importance as the layer was not intended to form during implantation in the first place [58–62]. The initial assumption was that that biological solution in a hip joint would adsorb protein molecules [63, 64]. Through the adsorption and triboactivity, the protein molecules denature, which means the proteins lose their shape and begin to degrade. Through hip simulators, the parameters that control the formation of tribofilms were investigated, usually with bovine calf serum as the lubricant. The tribofilm was shown to form on the CoCrMo alloys and UHMWPE, but not on Al<sub>2</sub>O<sub>3</sub> [59, 64, 65]. The investigation of the hip tribolayer formation has shown that both surface protein adsorption and change in proteins molecular weight occur. As the tribolayer forms, it is thought to simultaneously wear away, expelling particles [64, 66]. In explanted hips, the tribolayer was found to be between 30 and 40 nm by Buscher et al. [58]. To replicate this *in vitro*, the pressure (usually 30–200 MPa) and speed can be controlled to create films between 5 and 100 nm, with lower pressure and lower speed causing thicker films [63]. Another study demonstrated a range in thicknesses as a function of sliding speed (0–60 mm/s, 5 N), and categorized two film types. At low speed, a boundary layer of adsorbed protein molecules formed from aggregated protein molecules to form a gel. At high speed, the gel formed and then sheared to a thin film with a lower lubricant film thickness [67]. Contact of this protein phase is complex and dependent on a number of contact conditions and lubricant properties.

Further characterization in this field includes explant studies from patient hips, including light microscopy, SEM, TEM, EELS, EDS, XPS, and Raman spectroscopy [57, 68]. By investigating at the nanoscale, Liao et al. [57] characterized the articulating surfaces of explanted MoM replacement tribofilms, SEM shown in Fig. 3d. With Raman and EELS, it was determined the tribolayer was primarily carbon (95 %) and that the carbon was nano-graphitic (82 %), Raman shown in Fig. 4d and EELS shown in Fig. 5c [57–59]. Reproducing these results was attempted in simulators, but the carbon graphitic bonding was only 65 %, as opposed to 82 % in Liao et al. [66]. Even with explant analysis and simulator studies, there is no clear consensus on the tribolayer's impact on performance. The tribolayer can be considered beneficial because graphitic film would act as a solid lubricant, but there are also concerns of tribolayer degradation into tissue. Wimmer et al. [68] have shown reduced wear and electrochemical corrosion with the presence of the tribolayer, yet

Liao et al. [57] acknowledge that graphitic fragments could travel into cells to cause damage.

## 2.5 MEMS

Microelectromechanical systems are another nanofeatured, carbon-rich environment incorporating tribology, electrical activity, graphitic carbon films, and wear products. Nano-electromechanical or microelectromechanical systems (NEMS or MEMS) are devices that integrate mechanical and electrical functionality, and the mechanical function requires specific lubrication. MEMS have become common in consumer electronics accelerometers and in “lab on a chip” medical testing. MEMS are made using techniques of microfabrication, often pushing for smaller dimensions with new fabrication methods; with these length scales, typical lubricants cannot suffice [69]. A successful solution for MEMS longevity in applied devices has been using carbon film lubrication, especially vapor incorporation [70–72].

MEMS devices are successfully lubricated through use of carbon deposition that creates amorphous carbon films or through alcohol vapor that creates an adsorbed monolayer on the surface. The carbon deposition can create a wear film, shown in Fig. 3e [2], and the carbon-covered surface can become partially graphitic [73, 74]. Strawhecker et al. [70] found that linear alcohols between 1 and 10 carbon atoms long oxidized silicon at room temperature. At 10 % saturation of alcohol vapor, a monolayer was adsorbed, and by 90 % saturation, about 2–3 monolayers were adsorbed [70, 75]. It was shown that surface treatments of chemisorbed monolayers via functional groups, although initially reduced adhesion, did not survive mechanical contact [76, 77]. Carbon vapor, on the other hand, is seen to more permanently adsorb as a film, condense to a polymer, and act as a graphitic solid lubricant [74, 78–80]. A major advancement in vapor phase lubrication is that a hot surface is no longer needed to adsorb and decompose the carbon source to a carbon film [75, 81]. Now the driving force for bond passivation is the reactivity of the surface and the kinetics of the adsorption [69]. This method, compared to hydrophobic coating which seize after 3000 cycles, can run longer than 10<sup>8</sup> cycles with no evidence of wear, particle formation or changing operation characterized. An example of wear prevention is shown in Fig. 7, a MEMS switch lubricated with pentanol [82]. The enhanced performance comes from the graphitization of the adsorbed carbon through sliding. Furthermore, if the layer is worn, vapor in the device can repassivate the exposed surface for continuous lubrication [83].

MEMS lubrication has potential advancements as more complex defense and security applications require longer and tighter tolerances for performance, which means more



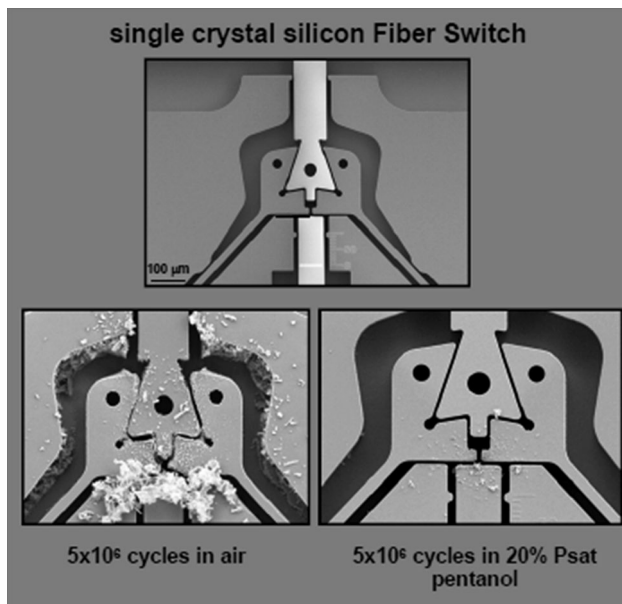


**Fig. 7** MEMS switch lubricated in air and pentanol, showing the buildup of wear when unlubricated [82]

cycles of reliable lubrication with minimal wear [69]. Single-component vapor species, however, have a vapor pressure that ranges by orders of magnitude over a narrow temperature range, where the necessary vapor for lubrication may instead become a condensed liquid. Additionally, filling a sealed volume with a known quantity of alcohol vapor presents some processing challenges for MEMS devices, as more control on vapor delivery and the possibility of polymer delivery design could be beneficial. By studying MEMS as a carbon lubricant system, the methods used for creating and characterizing these devices could be transferred to other triboactive systems, while other lubrication systems could help inspire the needed advancements for future MEMS designs.

## 2.6 Non-tribology: Catalysis Coke

By looking outside of tribology research, we can find similar nanographitic carbon films to inform carbon tribofilm systems. In catalysis, a parallel to graphitic tribolayers is seen in the formation of carbon coke. Coking is the accumulation of carbon-on-metal catalysts and supports through polymerization [84–86]. The process involves both chemical and physical bonding of carbon to form a film that eventually deactivates the catalyst. The process of coking has been studied thoroughly for reaction information, but can also be studied through the lens of carbon film composition and evolution [84, 85, 87]. Through studying a system with carbon, catalysis, and heat, but not tribology, mechanisms can be isolated for better understanding.

Similar to the reactions in tribochemistry, coke formation is considered a polymerization reaction, which forms surface coating carbon macromolecules. The reactions that lead to the film depend on the composition of the reaction mixture in addition to various reaction mechanism pathways. Through Raman spectroscopy, Li et al. [88] showed that polyaromatic and pre-graphitic species are predominant in zeolites, shown in Fig. 4e. Most coke research characterizes film as either polymerized [84, 89–91], pre-graphitic [88, 92], or graphitic [85, 93]. In addition to Raman spectroscopy, NMR [94], EELS [92], or X-rays [93, 95] are used to characterize the carbon bonding, with the EELS shown in Fig. 5 d measuring 83 % graphitic bonding [92]. Similar to tribofilms, there are often two types of coke described, an easy-to-remove initial formation and a difficult-to-remove carbon film. The difficult-to-remove coke has less hydrogen content and has developed into insoluble carbonaceous deposits [84, 94, 95].

In a catalyst, the structure of energetically favorable available sites can affect the allowable reactions and rate of the coke formation. This surface dependence is similar to the structural surface parameters affecting tribofilms during contact [90]. In the catalyst system, we see that reaction time, temperature, pressure, nature of the reactant, and operating conditions all affect coke formation [85]. Coke is also known to occur with gas reactions, where monolayers of carbon-containing molecules adsorb and react [86, 96]. Trimm et al. note that “carbon on catalysts behaves somewhat differently than graphite” [87, 97, 98], yet it may behave similarly to the nanographitic tribofilms. The important similarity is how the graphitic bonding evolves. There are similarities between coking in catalysts and triboactive systems, as triboactivity is only one factor in forming graphitic carbon films.

## 2.7 Other Examples: Cast Iron, Video Tape, Nanocomposite Coating

Carbon film generation is found in surprising places in the literature. We find that by looking beyond the initial search of “friction polymer” literature, more carbon films with striking triboactive and lubrication similarities are found. Here, we present three examples of carbon tribofilms that complement the discussion.

One example is research done on video tape recorders by Mizoh et al. [99] in the 1990s. This research examines the beneficial mild wear in video tape recorders (VTR) as high-speed rubbing on the magnetic tape produces a self-cleaning effect [99–102]. Without the wear, a polymer and brown stain form, which affects the reliability of the equipment. In the tribological system, the head factors, tape factors, and atmospheric factors are all found to determine formation of the tribolayer and whether wear

occurs [99]. The real contact area and the friction coefficient are considered as key design choices [99, 103]. The VTR system has a balance between the need for some wear for self-cleaning, but also the need to limit wear for longer head life. When humidity is high, the tribolayer causes film deterioration and is described as an easily removable, high molecular weight organic polymer with metal fragments; when humidity is low, the friction polymer formed sticks to the surface and reacts with the surface metal to cause seizure. It consists of iron, silicon, and carbon of about 500–700 Å thickness [100, 104]. These results echo the other fields discussed.

A second example is the glaze that forms during the run-in of cast iron. Cast iron is considered to have an important run-in period where smoothing of the surface and formation of a surface coating occurs [105]. The surface coating is considered to be derived primarily from the graphite present in the metal structure and the iron oxide,  $\text{Fe}_2\text{O}_4$ . The glaze is measured to be as thick as 1 mm and ranges in carbon content from 30 to 100 %, shown in Fig. 3f [105, 106]. The layer imparts a resistance to scuffing during the contact of mating surfaces, but just as importantly, it covers surface irregularities to produce a smoother surface [106]. This smoother surface allows higher loads to be carried by a fully hydrodynamic lubrication film without interaction of single asperities. An example of this used in industry is in internal combustion engine cylinder bores [105]. Montgomery et al. [105] consider that the carbon was “doubtless in the form of graphite” and also assume that there would be little to no thermal decomposition of the lubricating oil during the experiment. It was assumed that the carbon comes from the graphite in the cast iron and could not come from the lubrication oil [105, 107, 108]. These experiments from the 1960s help to show the evolution of the carbon film research and help to identify where assumptions were made.

It is now known that lubrication oil decomposition is indeed possible and can even start to be controlled [109]. This is demonstrated by a nanocomposite coatings patent [110]. The patent claims the production of a carbon lubricating film forming from deposits of a lubricating oil. The deposits form through reacting with the precisely designed nanocomposite active surface coating. The process of the lubricating film formation is remarkably similar to varnish formation, but in a more controlled way through the nanodesigned triboactive surface. The patented coating from Erdemir et al. [110] shows the design of a nanocomposite consisting essentially of a microstructural matrix of a catalytically active alloy of Cu, Ni, Pd, Pt, and Re. The lubricant is catalytically broken down and is disposed on the nanocomposite coating during sliding, as shown in Fig. 8a, b [110]. This carbon film was characterized through Raman spectroscopy, as shown in Fig. 8c

[110], and appears very similar to DLC films which are known to continue to develop graphitic bonding as they slide. With the current knowledge across fields, these examples from literature and patents can be further explored through experiments to develop the next generation of designed advantageous tribofilms.

### 3 Mechanisms of Formation

Now that the carbon film systems have been profiled, we describe mechanisms of the film formation. In the carbon film generating systems presented, the composition and structure of the films are shown to be similar, and the mechanism share similarities as well. Here, we present key mechanisms that have been proposed in the literature.

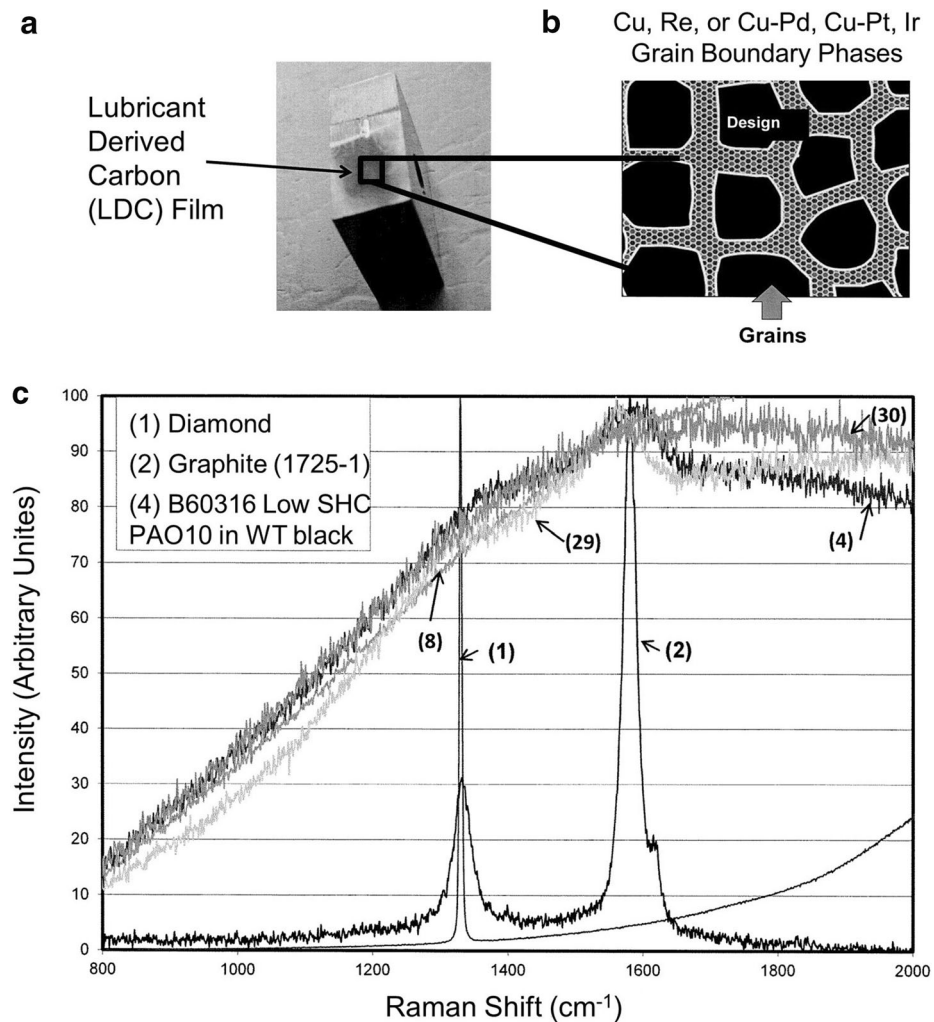
Some mechanisms, such as elevated localized heat, are frequently studied, whereas other contributors, like catalytic activity, have been researched thoroughly in some areas and seemingly forgotten in others. It is beneficial to study mechanisms, as some films are beneficial and some are harmful, and by finding differences in the mechanisms of formation, there is possibility to control film formation for advantageous properties. We lay out mechanisms by category, highlighting where seemingly disparate fields present parallel mechanisms, to show opportunity for future synergistic research.

#### 3.1 Pressure, Temperature, and Friction

All mechanisms of film formation have interplay and codependence. The most prominent contributors are localized increases in pressure, temperature, and friction. Cyclic sliding magnifies the effects. In these systems, local temperature spikes are due to single asperity friction or bubble collapse. Often in experimental setup, however, the entire system is elevated to simulate local heat. We address pressure, temperature, and friction together because they often cause one another. This triboactivity provides energy to induce graphitization.

As two surfaces come into contact with organic lubricant in-between, a system becomes tribochemically active. Friction occurs through the contact of nanoscale asperity features, and particularly, the point of contact has high frictional forces. In 1958, Hermance et al. [4] determined that “side to side motion was critical” for the organic deposit to form on metal surfaces in a benzene atmosphere. It is known for friction polymers that contact causes flash temperatures and high pressures [3]. In metal-on-metal hip implants, cyclic loading is thought to aid and accelerate the deposition process of protein films through increased protein–protein interaction, protein transport, and rearrangement of adsorbed proteins [67, 111]. Contact and shear

**Fig. 8** **a** Lubricant derived carbon film that forms during sliding on the nanocomposite surface, **b** design of the nanocomposite surface composition, and **c** Raman spectra of the film (indicated as 4 in the figure) presented with Raman spectra references of diamond (indicated with 1) and graphite (indicated with 2). United States Patent and Trademark Office [110]



forces contribute energy that allows lubricant molecules, whether proteins or hydrocarbons, to adsorb, react, and rearrange into a film. Friction at the surface, especially at the real contact area at single asperities, causes rupture of covalent bonds by frictional shearing [64]. Additionally, frictional forces are dependent on material and surface properties, as these factors also influence formation of tribolayers.

During asperity contact, high pressure and high temperature occur. The culprit is not overall system heat, but extreme pressures for small area and duration [4]. In particular, in varnish, heat is considered the major issue [40]. Both friction between metal surfaces and bubbles imploding within lubricant create enough heat to cause oil molecules to oxidize; oxidized molecules then lead to polymerization [39, 44]. The combination of oil-on-metal and metal-on-metal interactions can generate high temperatures and static charges that lead to spark discharge [40, 44]. In hydraulic systems, microdieseling is the implosion of entrained air bubbles when oil passes through

a high-pressure pump in a hydraulic circuit [44]. Air compression bubbles can reach at least 1000 °C and can produce low molecular weight hydrocarbons from oil, as degradation can easily occur in the 300–900 °C range [44, 45]. Similar to dieseling, adiabatic compressing can generate temperatures between 600 and 900 °C, while dark electrostatic discharge can cause temperature between 5,000 and 10,000 °C, whereas full spark discharge will generate a regular flash and nanosecond temperatures from 10,000 to 20,000 °C [40]. These data are primarily reported in trade publications by authors from the company Kleentek USA, yet research on hip implants and catalysis also report temperature as a key factor. Research on CoCrMo hip implants has shown that the mean temperature increased to 40–50 °C at the CoCrMo head and to 55 °C at the ZrO<sub>2</sub> head surface. For in vivo, the peak temperature from frictional heating in a total hip implant has been measured at 43.1 °C at the center of the joint's head [64]. The human albumin proteins are partly changed through the thermal denaturation at the sliding contact [64]. While

in catalysis, coke forms between 650 °C for the pyrolysis of hydrocarbons [98, 112]. Another study reports that polyolefinic and aromatic species form around 25–425 °C [88]. These thermal increases across systems from friction and pressure provide the energy needed to react the carbon into film with graphitic bonding.

### 3.2 Deposition and Adsorption

For systems with liquid lubricant, film formation begins with particles accumulating on the triboactive surfaces. Particles precipitate out of solution to form deposits on the surface; this is the precursor for the tribolayer [63, 64, 66]. Carbon-based lubricants go through chemical changes, due to pressure, heat, and friction, which cause chemical reactions. As the chemical products build up in solution, they agglomerate, polymerize, and drop out of solution. Polymerization will be further addressed the next section. The majority of research for deposition and adsorption come from varnish and hip tribolayer research.

In varnish, chemical reactions generate products that lead to new chemistry, different than the oil and its additives [113]. Oil degrades into micron size particles of higher molecular weight products that precipitate out of solution [42, 113]. Following precipitation, products deposit onto colder system surfaces such as cooler tanks and actuators. The low flow areas of the varnish circulation cause “soft” contaminants to form, whereas triboactive surfaces cause thin layers that harden over time [42]. Friction polymer research also describes the initial stages of polymer formation as “light colored and highly insoluble” deposits of saturated hydrocarbons [4]. Similarly in hip tribolayers, the proteins degrade by denaturing during triboactivity, and then deposit on sliding surfaces [64, 66, 67, 111]. This adsorption of albumin to one or both of the sliding surfaces is found to be a crucial factor for hip tribofilm formation. Furthermore, it is found for the hip tribolayer that metal and polymer surfaces will adsorb deposits, but  $\text{Al}_2\text{O}_3$  will not denature or adsorb albumin due to the hydrophilic surface [66, 114]. The local metallurgy of femoral heads could also cause preferential adsorption [19].

For vapor carbon sources, the first steps of the reactions are adsorption on the surface and then reactions yielding an observable deposit. An early study showed friction polymer formation from benzene lubrication [4]. During the “highly efficient process,” a monolayer of benzene was converted to a solid product after each pass over the surface. The adsorption step is crucial here; it was shown that an initial introduction of hydrogen would block deposit formation [4]. MEMS devices are also lubricated with alcohol vapor that adsorbs to the surface. The reactions can be measured through secondary ion mass spectroscopy

(SIMS). For a MEMS device, wear did not occur if the carbon vapor pressure was at least 8 % of the saturation pressure, or  $P/P_{\text{sat}} \geq 8\%$  [83, 115]. This saturation corresponds to a monolayer in coverage which created a lubricious environment that mitigated the friction and wear. Similarly with coke, the carbon source also comes from the air, and the carbon gas reactions happen when monolayers of carbon adsorb onto the catalyst and react into coke [96, 116]. The adsorbed carbon creates the carbon building blocks for tribofilms.

### 3.3 Polymerization and Organometallics

With the energy from heat and friction, carbon lubricants react, drop out of solution, deposit, and continue to polymerize. Discussion of high molecular weight species, oligomers, and polymerization is prevalent throughout research in friction polymers, varnish, hip tribolayers, MEMS, and catalysis. The friction polymer found on video-recording tape is even found to have a high molecular weight [99, 103]. The commonalities show that polymerization is key to forming graphitic films.

Early research on polymerization in friction polymers showed that high molecular weight species developed between lubricant and metal surface. Hermance et al. [4], studying metallic contacts in 1958, assumed the organic deposit was “a very thin layer of high molecular weight material” and that it was likely cross-linked with little oxygen in the molecule [4]. Later in the 1970s, Hsu and Klaus used gel permeation chromatography to identify the presence of high molecular weight species, including organo-iron species [15, 16]. The species were identified as high molecular weight organometallic polymers of variable molecular weights (10,000–100,000 MW) [7, 39].

Across systems, high molecular weight polymers are present. In varnish, the formation begins with the condensation and polymerization to form high molecular weight oligomers and the agglomeration of insoluble partings on metal surfaces [39, 42]. In the hip tribolayer, the transformation of protein to graphitic carbon film is explained by first showing that lower molecular bands were formed during mechanical denaturation through rupture of covalent bonds in human serum albumin by frictional shearing motion [64]. The denatured proteins adsorb on the metal surface, forming a gel-like layer of higher molecular weight. This gel reacts into a graphitic tribolayer, which acts as a solid lubricant [67]. Similarly in MEMS, a high molecular weight product forms on the contacts, and it has been shown that “higher” alcohols ( $4 < n < 11$ ) reduce friction and cause low-wear rate as compared to the lower alcohols ( $n < 4$ ) [117]. This would support the idea that they could polymerize to high molecular weight species, which could form a lubricating tribolayer [69]. It is



postulated for MEMS that metal alkoxides condense to a polymer and act as lubricant, showing another example of the intertwined roles of oxidation, organometallics, and polymerization [80]. Coke on catalyst formation can also be considered a kind of condensation–polymerization reaction, resulting in macromolecules [87]. Often the initial hydrogenated carbon molecules are characterized to be  $\text{CH}_x$  with  $x$  varying in studies to be  $0.5 < x < 1$  [118], or  $1 < x < 3$  [95], or  $x = 2$  [91]. XAES spectra indicate that with longer reaction time, the hydrogenated carbon dehydrogenate slowly to amorphous or graphitic carbon [118]. The pathway to coke from olefins or aromatics can involve polymerization, cyclization to form benzenes, and formation of polynuclear aromatics [86, 89, 90, 119]. This transformation in polyaromatic carbon makes the film less reactive and difficult to remove [95, 98, 112]. Polymerization seems to present as the key step between carbon building blocks and graphitic film.

Organometallic formation is a step in the process of tribolayer formation. In friction polymers, the role of organometallics has been shown on a variety of metal surfaces to accelerate the rate of hydrocarbon oxidation [16]. It has been found that dynamic wear tests at room temperature form oil-soluble, metal-containing compounds [3], which are primarily high molecular weight organometallics [3]. Organometallic compounds have a relative molecular mass ranging from 100 to 100,000 MW. The carboxylic acids formed from hydrocarbon oxidation are proposed to react with the metal surface and two hydrogen atoms to form conjugated double bonds [14]. This shows a possible pathway for multi-elemental lubricant to become a primarily carbon film. In iron alloys, organometallic compounds are formed between the iron surface and base oil and are considered essential to lubrication as this surface activity is part of the dominant tribochemical reaction. Similarly, CoCr alloys form organometallic layers during wear, showing that this is a possible mechanism inside the hip MoM contact as well [66, 120, 121].

### 3.4 Catalytic Activity and Fresh Surfaces

Catalytic activity is another step of the reaction process that helps explain how these tribochemical reactions are possible. In the case of coking on an intentional catalyst, the catalytic elements are obvious, and in the case of a triboactive system, exposure of fresh surfaces can provide the catalytic activity. By looking at similarities between triboactive systems and coke, we can begin to isolate mechanisms and see how many steps are influential to form the carbon films seen across these systems.

Metal surfaces have been noted for their role in tribofilm formation from the early studies in the 1950s–1970s. Hermande et al. [4] noted that the surface was an “active metal”

and the reaction would come to a standstill when it was completely covered with tribofilms or if hydrogen was incorporated in the chamber. Klaus et al. found that a variety of metal surfaces accelerated the rate the hydrocarbon oxidation, concluding that metal reacts directly the organic lubricant to form metal salts [3, 16]. Nascent iron surfaces were shown to react with hydrocarbon molecules to form smaller molecular fragments, with the carbon source being liquid or gas [9, 11, 15]. Iron and steel are often studied [9, 15]; early studies noted that palladium, molybdenum, tantalum, and chromium can form the carbon tribofilms as well [4].

In addition to metals, semiconductors and insulators can cause tribochemical reactions as well. When a new surface is created, residual electric charges can become active because of disrupted surface bonds [122–124]. For crystalline solids, dangling bonds have been observed as the major surface active site for reactions [17, 125, 126]. The surface chemical reactivity for these classes of solids can be dominated by defect sites and dangling bonds, especially when heated to bond dissociation temperatures or mechanically disrupted.

By looking at pure catalysts, we can discover that adsorption, polymerization, and graphitization can all occur with the encouragement of catalytic activity instead of with friction. Carbon gas reactions occur where monolayers of carbon adsorb and react on the catalyst surface [88, 96]. Metal catalysts yield olefins, which polymerize on the acidic sites of the support and then stabilize through dehydrogenation [84, 90]. The presence of catalytic elements in all the reviewed systems, even in small quantities as alloys, explains how catalytic activity provides energy pathways for graphitic film formation.

### 3.5 Graphitization

The process of graphitization, amorphous carbon turning to graphitic ordered carbon, is a well-studied phenomenon that is a key process in the formation of carbon tribolayers. Amorphous carbon deposits are often thermodynamically unstable, and when external thermal energy is provided, the atoms begin to rearrange and assume more thermodynamically stable bonding configurations, i.e., partially graphitic structures which contain more  $\text{sp}^2$  bonding. While the end point may be an ordered graphite structure, more common is a disordered matrix with nanoscale regions of graphitic bonding. In DLC or diamond systems, this process is a rehybridization of the carbon–carbon bonds, but when the starting materials are oils, waxes, or proteins, it is an oxidation since carbon–hydrogen or similar bonds are being converted to  $\text{sp}^2$  carbon–carbon bonds. The graphitization process often turns a carbon-containing film into a solid lubricant.

The tribochemical reactions between amorphous carbon sliding surfaces cause low-friction tribofilms to form [127, 128]. For DLC films, graphitization, sometimes explained as rehybridization, is often investigated in as DLC become more lubricating during sliding because the amorphous film turns partially graphitic [31, 32]. Heat and catalytic activity can also turn amorphous carbon to graphitic, but in most of these systems tribochemical contributions are most significant. Tribochemical transitions are mechanochemically active; amorphous atoms change position as they react [29]. Recent concepts of tribocharging, tribomicroplasma generation, and triboemission phenomena have been proposed to contribute to graphitization as well [129].

By looking at these systems together, we can find connections between the prominent DLC research and details found in other fields. For most DLC films, Raman spectroscopy and electron diffraction can show disordered graphite structure in transfer layers [27, 130–133]. For MEMS, graphitization is seen in parts fabricated of amorphous diamond, which produce a low-wear, DLC-like film. High-cycle varnish areas are found to be graphitic, as shown in the varnish Raman and EELS data, which point to tribochemical contributions (probably oxidative) causing graphitization in this system as well [39]. In coke, the process of carbon oligomers dehydrogenating to amorphous carbon and then to graphitic carbon is described by XANES measurements over time [95]. The graphitic content of carbon films is an important aspect, as this quality influences lubrication properties.

### 3.6 Nanoparticles and Metal Particles

The influence of wear and wear particles is often mentioned in carbon films research, but the ties to a mechanism of formation are not directly clear. Carbon nanoparticles form in varnish, starting at 10–2000 nm, but they are difficult to measure with standard industry practice [42]. In industry, the aim is to prevent and control these very small carbon-based particles through improved cleanliness monitoring, as the particles are thought to increase wear. These particles are most likely the initial form of the condensing polymers before aggregation, but research suggests that they influence lubrication in a different way when they are still soluble as opposed to once they deposit.

Metal nanoparticles are included in some system analysis, mostly in MoM hip or iron-based systems. In hip simulator experiments, the film created was organometallic in nature, containing a number of embedded particles. The particles in the film were smaller and smoother in morphology than those typically ejected from the bearing [64, 66]. The hip simulator experiments show that metallic particles may cause the initial protein denaturation. This

would indicate that metallic particles are a precursor to tribolayer formation, yet this conclusion is not definitive [66]. Furthermore, in cast iron glaze, iron oxide nanoparticles are found in the run-in layer and considered to be a key component generated during wear and then tribolayer formation [105]. The presence of nanoparticles creates additional triboactive surfaces as they act as third body particles. It is not conclusive whether there is a specific mechanistic role of nanoparticles in tribofilm formation.

## 4 Discussion

After introducing key carbon film systems and breaking down the mechanism that cause film formation, we discuss particular similarities, reaction thermodynamics, and future opportunities.

### 4.1 Similarities

The systems summaries and mechanisms explanation present substantial evidence of similarities between these carbon films. There are similarities in appearance, chemical composition, chemical reactions, and influence on performance. The presence of carbon films has been heavily tied to performance—both good, detrimental, and mixed—yet film characterization provides insight that applies across systems.

The notable parallels begin with descriptions and word choice across fields. Friction polymers and varnish are noted to appear initially pale yellow and darken in time, often described as dark reddish brown and sometimes shiny [4, 10, 42, 44]. Even the early friction polymer from Hermance et al. [4], once heated, was said to resemble a “coke-like residue”. Beyond appearance, the dual formation of the carbon films was noted across systems—in friction polymer, varnish, MoM hips, and coking—as both having an easily removable carbon film and a more adhered form as well [6, 44, 67, 88]. This description, along with proposed mechanisms across these systems, seems to point to initial globular polymerized deposits versus the further-reacted, graphitized films. With these similar mechanisms, there are even parallel reaction diagrams, showing organic precursors turning into pre-graphitic condensation products in friction polymers and in catalysis, as shown in Fig. 9a [134] and 9b [135], respectively. These parallel formation theories from vastly different fields are striking.

### 4.2 Thermodynamics

It is clear that the carbonaceous material from friction polymers, DLC, varnish, hip implants, MEMS, and catalytic coking share striking similarities. Something general

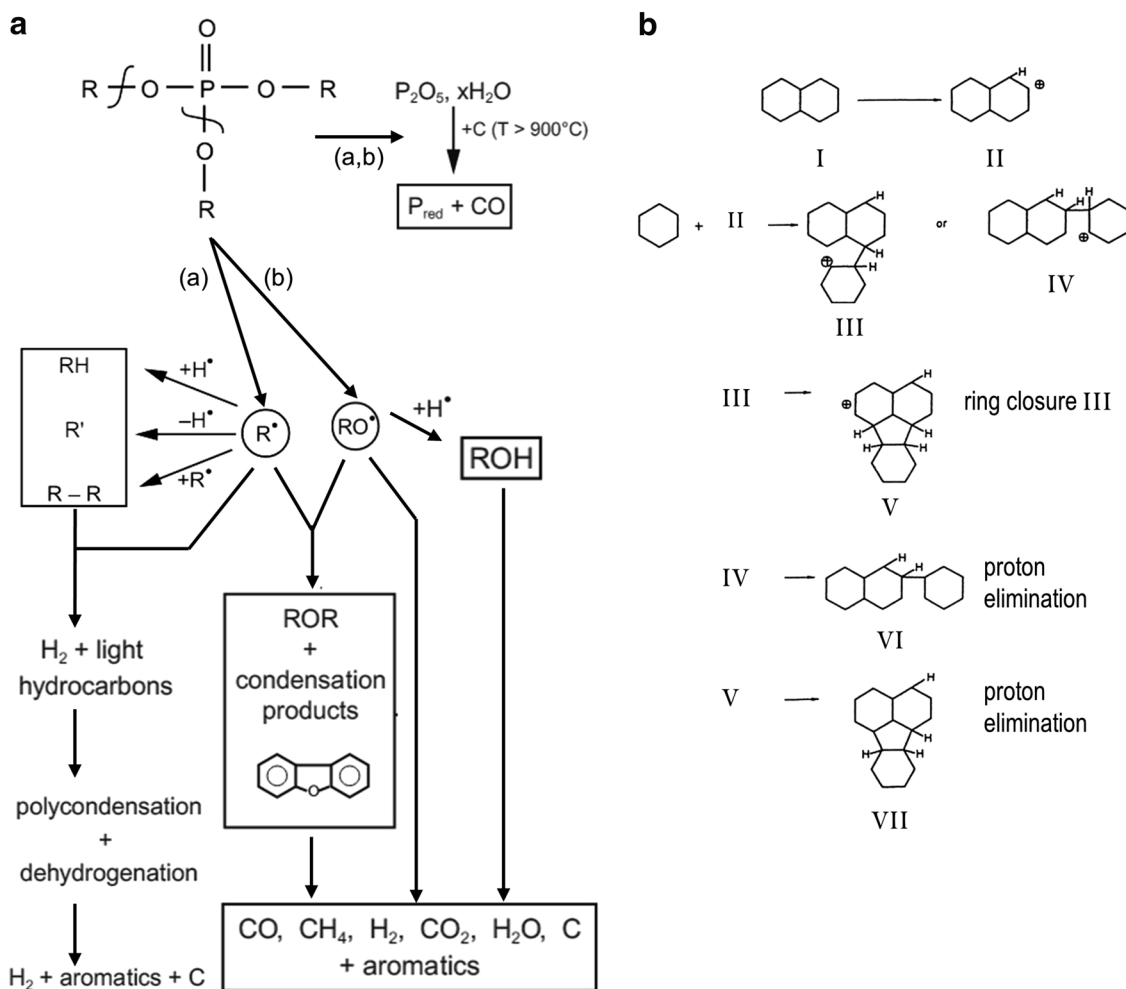


**Fig. 9** Similarities in reaction diagrams showing organic precursors turning into pre-graphitic condensation products in friction polymers and coke. **a** For a friction polymer, general pyrolysis scheme of

phosphates through thermal degradation [134]. **b** For coking, carbonium ion mechanism for formation of higher aromatics from benzene and naphthalene [135]

is taking place—what? A phase map of carbon structures from the literature, shown in Fig. 10 [53], provides important clues whether we superimpose the approximate positions of amorphous carbon, proteins, oil products, and graphite [21]. Through heat, friction, catalytic activity, or some combination, the carbon  $sp^3$  bonding shifts to  $sp^2$  graphitic bonding, coupled with loss of hydrogen and other elements as volatile gases or liquids such as water and carbon dioxide.

Experimental demonstrations can show how heat and sliding can both individually contribute to graphitization, which mirrors the thermodynamic evolution in different systems. A DLC study by Wu et al. [31] annealed DLC films at different temperatures and then used Raman spectroscopy to characterize the graphitization at various temperatures. In Fig. 11 a, it was shown that as the anneal temperature increases, the hydrogen was driven away and the formation of  $sp^2$  bonding or graphitic microcrystallites

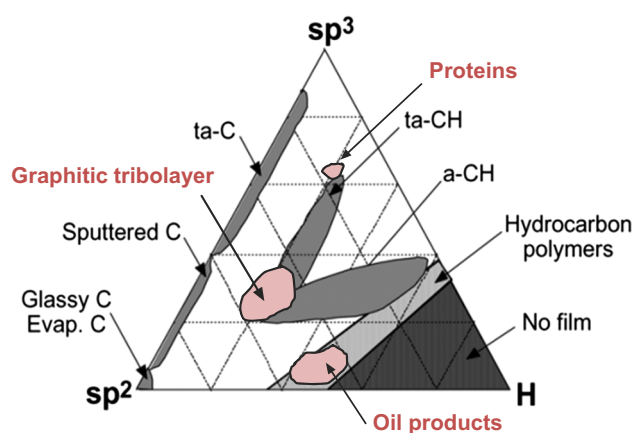
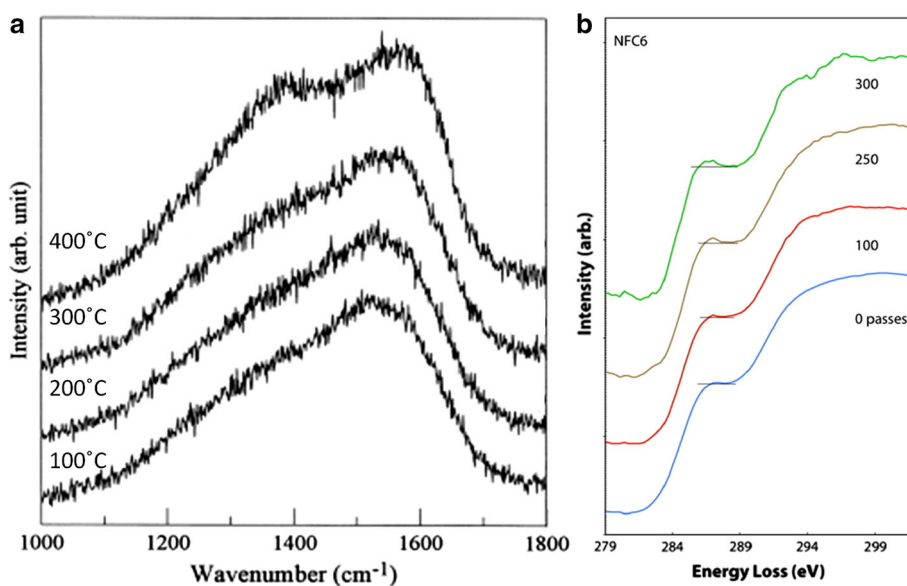


**Fig. 10** Ternary phase map based upon for various carbon films [53], including proposed approximate placement for proteins and oil lubricants, which shows their respective  $sp^2$ ,  $sp^3$ , and hydrogen contents. This provides a map of the dynamic change of these materials into graphitic films

**Fig. 11** Examples of input energy causing graphitization in DLC and NFC carbon films.

**a** At increasing heat treatment temperatures, DLC film became increasingly graphitic, measured by Raman spectroscopy [31].  
**b** During in situ sliding, NFC film became more graphitic measured by EELS [136]



began [31]. For comparison, in an experiment on nearly frictionless carbon by Merkle et al. [136], carbon film underwent sliding with EELS measurements documenting increasing graphitic bonding, shown in Fig. 11b. The energetic input does not matter, the carbon composition reacts toward the lowest carbon form, graphitic bonding.

To further explain the possible reaction pathways, the carbon systems can be analyzed from the point of open system thermodynamics. Lubricant oils, proteins, and other carbon sources react to become primarily carbon in composition; the other elements become volatile products such as water and carbon monoxide. The driving force—heat, friction, or a combination—plus coming into contact with a catalytic metal surface increases the reaction constant by decreasing the activation barrier for  $sp^2$  bonding. The probability that the bonding will shift from amorphous to graphitic can be calculated by

$$P(s) = \exp\left(\frac{-(E - \sigma * C)}{kT}\right)$$

where  $E$  is the energy barrier,  $\sigma$  is the stress applied,  $C$  is a constant,  $k$  is the Boltzmann constant, and  $T$  is temperature. We can compare a system at room temperature with an applied stress and a system at high temperatures with no applied stress to explain the stress-assisted graphitization of carbon. We can assume an energy barrier on the order of 1 eV for the amorphous carbon to graphitic transition [137, 138] and 40 MPa for the applied stress similar to a hip implant or machine applied to a volume of  $2 \text{ \AA} \times 2 \text{ \AA} \times 2 \text{ \AA}$  [139]. Graphitization can occur at 1500 K with no stress and can occur around room temperature with assisted stress, although at a rate of about 5000 times slower. This model agrees with our observations across systems.

### 4.3 Future Opportunities

Connecting these fields of research could begin to answer why some films are advantageous and others are not. Friction polymers can be designed to be beneficial, yet small changes can degrade system performance. Changes such as film thickness or particle generation take a friction polymer outside the design tolerances. Machine tolerances may be why the varnish tribolayer is considered detrimental, as varnish is often uneven and inhomogeneous. It is deposited without intention, outside of the parameters of the machine. The hip tribolayer is also unintentional, yet it is experimentally theorized to be protective. By studying the formation of the two tribolayers together, beneficial tribolayers can be designed to form, similar to the patented nanocomposite system. Further opportunities come from understanding commonalities in the formation mechanisms. Both MEMS and friction polymer fields study the film formation differences between metal and organic substrates, connecting how the substrate leads to an effective film. Both metal hips and varnish deal with static charge that leads to spark discharge, and by studying the metal-on-metal contacts, it could be mitigated or controlled in both systems [40, 44]. For film formation, MEMS, cast iron, and nanocomposite coatings all need a reservoir or carbon to begin and continue their formation, yet this evolution is not well understood [69, 105, 110]. Cast iron graphitic layers do not only act as a solid lubricant, but also as a cover to single asperities; these layers can inspire other film designs [105]. Additionally, there are carbon film systems not addressed here, possibility very specific to a field; those carbon films could be analyzed or applied across discipline for novel outcomes. Other forms of partially graphitic carbon, such as glassy carbon, could also be



beneficial for comparison. These possible research connections can lead to improved design for better performance.

Mutually beneficial information can be exchanged through collaborative monitoring, characterization, and design techniques. For example, the multivariable analysis of SIMS used in MEMS analysis allows for rapid identification of subtle changes in chemistry. SIMS could be used for chemical evolution measurements of friction polymers to expand beyond the current steel–hydrocarbon system knowledge [115]. In varnish work, nanoparticle-tracking analysis requires particle detection between 10 and 2000 nm, yet this work is complex and expensive, outside of the usual scope of varnish monitoring [39, 42]. In academic laboratories, however, nanoscale characterization and monitoring is becoming standard. Through collaboration, research on varnish could also inform the work on nanoparticle condensation polymers that occur in friction polymers, hips tribolayers, and other systems. Through cross-field research, designing controlled catalytic surfaces could lead to engineered varnish films as beneficial lubricants.

## 5 Conclusions

- Notable carbon films are present in many fields. The systems of friction polymers, diamond-like carbon (DLC) coatings, varnish from industrial lubricants, the tribolayer from metal-on-metal (MoM) hip replacements, microelectromechanical systems (MEMS), and catalysis coke produce similar graphitic carbon films. Graphitic carbon films can be a helpful solid lubricant or can form a damaging deposit.
- Key mechanisms of formation of graphitic carbon films include pressure, temperature, and friction; deposition and absorption; polymerization and organometallics; catalytic activity; graphitization; and particle interaction. The energy inputs to a system, through heat, friction, or catalysis, causes graphitization. The result is often regions of nanographitic bonding, creating a partially graphitic film.
- Through integrating research approaches, cross-field collaboration can allow for innovative developments. Creativity comes from bridging disciplines: a good idea from one discipline can be an innovate idea when applied to another.

**Acknowledgements** This work was funded by the NSF under the Grant Number CMMI-1030703. EEH is funded through the National Defense Science and Engineering Graduate Fellowship.

## References

1. Gangopadhyay, A., McWatt, D., Zdrodowski, R., Liu, Z., Elie, L., Simko, S., Erdemir, A., Ramirez, G., Cuthbert, J., Hock, E.: Development of modified PAG (polyalkylene glycol) high VI high fuel efficient lubricant for LDV applications (2014)
2. Tanner, D.M., Smith, N.F., Irwin, L.W., Eaton, W.P., Helgesen, K.S., Clement, J.J., Miller, W.M., Miller, S.L., Dugger, M.T., Walraven, J.A.: MEMS reliability: infrastructure, test structures, experiments, and failure modes. In: Sandia National Labs., Albuquerque, NM (US); Sandia National Labs., Livermore, CA (US) (2000)
3. Hsu, S.M., Gates, R.S.: Effect of materials on tribochemical reactions between hydrocarbons and surfaces. *J. Phys. D Appl. Phys.* **39**(15), 3128–3137 (2006). doi:[10.1088/0022-3727/39/15/S02](https://doi.org/10.1088/0022-3727/39/15/S02)
4. Hermance, H.W., Egan, T.F.: Organic deposits on precious metal contacts. *Bell Syst. Tech. J.* **37**(3), 739–776 (1958). doi:[10.1002/j.1538-7305.1958.tb03885.x](https://doi.org/10.1002/j.1538-7305.1958.tb03885.x)
5. Antler, M.: Tribology of metal coatings for electrical contacts. *Thin Solid Films* **84**(3), 245–256 (1981). doi:[10.1016/0040-6090\(81\)90022-5](https://doi.org/10.1016/0040-6090(81)90022-5)
6. Furey, M.J.: The formation of polymeric films directly on rubbing surfaces to reduce wear. *Wear* **26**(3), 369–392 (1973). doi:[10.1016/0043-1648\(73\)90188-9](https://doi.org/10.1016/0043-1648(73)90188-9)
7. Gates, R.S., Jewett, K.L., Hsu, S.M.: A study on the nature of boundary lubricating film: analytical method development. *Tribol. Trans.* **32**(4), 423–430 (1989). doi:[10.1080/10402008908981909](https://doi.org/10.1080/10402008908981909)
8. Hsu, S.M.: Fundamental mechanisms of friction and lubrication of materials. *Langmuir* **12**(19), 4482–4485 (1996). doi:[10.1021/la9508856](https://doi.org/10.1021/la9508856)
9. Morecroft, D.W.: Reactions of octadecane and decoic acid with clean iron surfaces. *Wear* **18**(4), 333–339 (1971). doi:[10.1016/0043-1648\(71\)90076-7](https://doi.org/10.1016/0043-1648(71)90076-7)
10. Chaikin, S.W.: On frictional polymer. *Wear* **10**(1), 49 (1967). doi:[10.1016/0043-1648\(67\)90106-8](https://doi.org/10.1016/0043-1648(67)90106-8)
11. Mori, S., Imaizumi, Y.: Adsorption of model compounds of lubricant on nascent surfaces of mild and stainless steels under dynamic conditions. *Tribol. Trans.* **31**(4), 449–453 (1988). doi:[10.1080/10402008808981847](https://doi.org/10.1080/10402008808981847)
12. Herrera-Fierro, P., Shogrin, B.A., Jones, W.R.: Spectroscopic analysis of perfluoropolyether lubricant degradation during boundary lubrication. *Lubr. Eng.* **56**(2), 23–29 (2000)
13. Zhang, J., Demas, N.G., Polycarpou, A.A., Economy, J.: A new family of low wear, low coefficient of friction polymer blend based on polytetrafluoroethylene and an aromatic thermosetting polyester. *Polym. Adv. Technol.* **19**(8), 1105–1112 (2008). doi:[10.1002/pat.1086](https://doi.org/10.1002/pat.1086)
14. Hsu, S.M., Klaus, E.E., Cheng, H.S.: A mechano-chemical descriptive model for wear under mixed lubrication conditions. *Wear* **128**(3), 307–323 (1988). doi:[10.1016/0043-1648\(88\)90066-X](https://doi.org/10.1016/0043-1648(88)90066-X)
15. Hsu, S.M., Klaus, E.E.: Estimation of the molecular junction temperatures in four-ball contacts by chemical reaction rate studies. *ASLE Trans.* **21**(3), 201–210 (1978). doi:[10.1080/05698197808982875](https://doi.org/10.1080/05698197808982875)
16. Hsu, S.M., Klaus, E.E.: Some chemical effects in boundary lubrication part I: base oil-metal interaction. *ASLE Trans.* **22**(2), 135–145 (1979). doi:[10.1080/05698197908982909](https://doi.org/10.1080/05698197908982909)
17. Lenahan, P.M., Curry, S.E.: First observation of the 29Si hyperfine spectra of silicon dangling bond centers in silicon nitride. *Appl. Phys. Lett.* **56**(2), 157 (1990). doi:[10.1063/1.103278](https://doi.org/10.1063/1.103278)

18. Schmellenmeier, H.: Die Beeinflussung von festen Oberflächen durch eine ionisierte. *Exp. Tech. Phys.* **1**, 49–68 (1953)
19. Aisenberg, S.: Ion-Beam Deposition of Thin Films of Diamondlike Carbon. *J. Appl. Phys.* **42**(7), 2953 (1971). doi:[10.1063/1.1660654](https://doi.org/10.1063/1.1660654)
20. Eryilmaz, O.L., Erdemir, A.: TOF-SIMS and XPS characterization of diamond-like carbon films after tests in inert and oxidizing environments. *Wear* **265**(1–2), 244–254 (2008). doi:[10.1016/j.wear.2007.10.012](https://doi.org/10.1016/j.wear.2007.10.012)
21. Erdemir, A., Donnet, C.: Tribology of diamond-like carbon films: recent progress and future prospects. *J. Phys. D Appl. Phys.* **39**(18), R311–R327 (2006). doi:[10.1088/0022-3727/39/18/R01](https://doi.org/10.1088/0022-3727/39/18/R01)
22. Singh, H., Ramirez, G., Eryilmaz, O., Greco, A., Doll, G., Erdemir, A.: Fatigue resistant carbon coatings for rolling/sliding contacts. *Tribol. Int.* (2016). doi:[10.1016/j.triboint.2016.02.008](https://doi.org/10.1016/j.triboint.2016.02.008)
23. Lawes, S.D.A., Fitzpatrick, M.E., Hainsworth, S.V.: Evaluation of the tribological properties of DLC for engine applications. *J. Phys. D Appl. Phys.* **40**(18), 5427–5437 (2007). doi:[10.1088/0022-3727/40/18/S03](https://doi.org/10.1088/0022-3727/40/18/S03)
24. Grill, A.: Tribology of diamondlike carbon and related materials: an updated review. *Surf Coat Tech* **94–5**(1–3), 507–513 (1997). doi:[10.1016/S0257-8972\(97\)00458-1](https://doi.org/10.1016/S0257-8972(97)00458-1)
25. Lettington, A.H.: Applications of diamond-like carbon thin films. *Carbon* **36**(5–6), 555–560 (1998). doi:[10.1016/S0008-6223\(98\)00062-1](https://doi.org/10.1016/S0008-6223(98)00062-1)
26. Hauert, R.: A review of modified DLC coatings for biological applications. *Diam. Relat. Mater.* **12**(3–7), 583–589 (2003). doi:[10.1016/S0925-9635\(03\)00081-5](https://doi.org/10.1016/S0925-9635(03)00081-5)
27. Erdemir, A., Bindal, C., Pagan, J., Wilbur, P.: Characterization of transfer layers on steel surfaces sliding against diamond-like hydrocarbon films in dry nitrogen. *Surf. Coat. Tech.* **76–77**(1–3), 559–563 (1995). doi:[10.1016/0257-8972\(95\)02518-9](https://doi.org/10.1016/0257-8972(95)02518-9)
28. Ponsoonnet, L., Donnet, C., Varlot, K., Martin, J.M., Grill, A., Patel, V.: EELS analysis of hydrogenated diamond-like carbon films. *Thin Solid Films* **319**(1–2), 97–100 (1998). doi:[10.1016/S0040-6090\(97\)01094-8](https://doi.org/10.1016/S0040-6090(97)01094-8)
29. Pastewka, L., Moser, S., Gumbsch, P., Moseler, M.: Anisotropic mechanical amorphization drives wear in diamond. *Nat. Mater.* **10**(1), 34–38 (2011). doi:[10.1038/Nmat2902](https://doi.org/10.1038/Nmat2902)
30. Moon, M.W., Jensen, H.M., Hutchinson, J.W., Oh, K.H., Evans, A.G.: The characterization of telephone cord buckling of compressed thin films on substrates. *J. Mech. Phys. Solids* **50**(11), 2355–2377 (2002). doi:[10.1016/S0022-5096\(02\)00034-0](https://doi.org/10.1016/S0022-5096(02)00034-0)
31. Wu, W.J., Hon, M.H.: Thermal stability of diamond-like carbon films with added silicon. *Surf. Coat. Tech.* **111**(2–3), 134–140 (1999). doi:[10.1016/S0257-8972\(98\)00719-1](https://doi.org/10.1016/S0257-8972(98)00719-1)
32. Scharf, T.W., Singer, I.L.: Role of third bodies in friction behavior of diamond-like nanocomposite coatings studied by in situ tribometry. *Tribol. Trans.* **45**(3), 363–371 (2002). doi:[10.1080/10402000208982561](https://doi.org/10.1080/10402000208982561)
33. Savage, R.H.: Graphite lubrication. *J. Appl. Phys.* **19**(1), 1–10 (1948). doi:[10.1063/1.1697867](https://doi.org/10.1063/1.1697867)
34. Rabinowicz, E., Imai, M.: Frictional properties of pyrolytic boron nitride and graphite. *Wear* **7**(3), 298–300 (1964). doi:[10.1016/0043-1648\(64\)90092-4](https://doi.org/10.1016/0043-1648(64)90092-4)
35. Fusaro, R.L., Sliney, H.E.: Graphite fluoride (CF<sub>x</sub>)<sub>n</sub>—a new solid lubricant. *ASLE Trans.* **13**(1), 56–65 (1970). doi:[10.1080/05698197008972282](https://doi.org/10.1080/05698197008972282)
36. Kato, K., Umehara, N., Adachi, K.: Friction, wear and N2-lubrication of carbon nitride coatings: a review. *Wear* **254**(11), 1062–1069 (2003). doi:[10.1016/S0043-1648\(03\)00334-x](https://doi.org/10.1016/S0043-1648(03)00334-x)
37. Shen, Y., Xu, J.J., Jin, M., Wang, J.J., Wang, L., Han, X.G., Zhang, H.P., Zhang, Y.D.: Tribological behavior among piston ring-hydrorefined mineral oil-cylinder liner for diesel engine. *Appl. Mech. Mater.* **148**, 1307–1311 (2012)
38. Johnson, M., Spurlock, M.: Strategic oil analysis: estimating remaining lubricant life. *Tribol. Lubr. Technol.* (2010)
39. Livingstone, G., Oakton, D.: The emerging problem of lubricant varnish. *Maint. Asset Manage.* **25**, 38–42 (2010)
40. Lucas, L.: Problems and sources of varnish in hydraulic fluid. *Hydraul Pneum.* (2007)
41. Sasaki, A., Uchiyama, S., Kawasaki, M.: Varnish formation in the gas turbine oil systems. *J. ASTM Int.* **5**(2), 1–12 (2008)
42. Phillips, W.D., Staniewski, J.W.G.: The origin, measurement and control of fine particles in non-aqueous hydraulic fluids and their effect on fluid and system performance. *Lubr. Sci.* **28**(1), 43–64 (2016). doi:[10.1002/ls.1300](https://doi.org/10.1002/ls.1300)
43. Atherton, B.: How to stop varnish before it costs you. *Plast. Today* (2008)
44. Atherton, B.: Discovering the root cause of varnish formation. *Pract. Oil Anal.* (2007)
45. Phillips, W.D.: The high-temperature degradation of hydraulic oils and fluids©. *J. Synth. Lubr.* **23**(1), 39–70 (2006). doi:[10.1002/jsl.11](https://doi.org/10.1002/jsl.11)
46. Sasaki, A., Uchiyama, S., Yamamoto, T.: Generation of static electricity during oil filtration. *Lubr. Eng.* **55**(9), 14–21 (1999)
47. Barber, A., Filippini, B., Profflet, R., Tam, N.: A Fluid solution to preventing varnish formation in hydraulic systems. In: *Lubricants Symposium 2008*, pp. 175–175 (2008)
48. Ribeiro, N.M., Pinto, A.C., Quintella, C.M., da Rocha, G.O., Teixeira, L.S.G., Guarieiro, L.L.N., Rangel, M.D., Veloso, M.C.C., Rezende, M.J.C., da Cruz, R.S., de Oliveira, A.M., Torres, E.A., de Andrade, J.B.: The role of additives for diesel and diesel blended (ethanol or biodiesel) fuels: a review. *Energy Fuels* **21**(4), 2433–2445 (2007). doi:[10.1021/ef070060r](https://doi.org/10.1021/ef070060r)
49. Heo, G., Lee, S., Kim, H., Park, U., Lee, G., Han, D., Chu, M., Choi, U., Hur, K., Lee, S.G., Kim, H.S., Park, W.K., Lee, K.C., Han, D.H., Chu, M.K., Choi, W.J.: Varnishing processing unit for processing surface of workpiece, has circulating pump provided with nozzle in which hydro static ball pressurizes exterior of workpiece, where circulating pump supplies hydraulic fluid to varnishing tool. KR2010095230-A; KR1077093-B1
50. Hum, W., Holt, D.G.L., Blumenfeld, M.L., Galiano-Roth, A.S.: Improving varnish control in a mechanical device requiring hydraulic fluids, turbine oils, industrial fluids, circulating oils, or combinations by supplying the mechanical device with a lubricating composition. US2015099675-A1; WO2015050690-A1
51. ASTM: Standard test method for measurement of lubricant generated insoluble color bodies in in-service turbine oils using membrane patch colorimetry. In: *ASTM International, West Conshohocken. vol. ASTM D7843-12. ASTM International* (2012)
52. Robertson, J.: Diamond-like amorphous carbon. *Mater. Sci. Eng. R* **37**(4–6), 129–281 (2002). doi:[10.1016/S0927-796x\(02\)00005-0](https://doi.org/10.1016/S0927-796x(02)00005-0)
53. Ferrari, A.C., Robertson, J.: Interpretation of Raman spectra of disordered and amorphous carbon. *Phys. Rev. B* **61**(20), 14095–14107 (2000). doi:[10.1103/PhysRevB.61.14095](https://doi.org/10.1103/PhysRevB.61.14095)
54. Chu, P.K., Li, L.H.: Characterization of amorphous and nanocrystalline carbon films. *Mater. Chem. Phys.* **96**(2–3), 253–277 (2006). doi:[10.1016/j.matchemphys.2005.07.048](https://doi.org/10.1016/j.matchemphys.2005.07.048)
55. Pappas, D.L., Saenger, K.L., Cuomo, J.J., Dreyfus, R.W.: Characterization of laser vaporization plasmas generated for the deposition of diamond-like carbon. *J. Appl. Phys.* **72**(9), 3966–3970 (1992). doi:[10.1063/1.352249](https://doi.org/10.1063/1.352249)
56. Cuomo, J.J., Pappas, D.L., Bruley, J., Doyle, J.P., Saenger, K.L.: Vapor deposition processes for amorphous carbon films with sp<sup>3</sup> fractions approaching diamond. *J. Appl. Phys.* **70**(3), 1706–1711 (1991)
57. Liao, Y., Pourzal, R., Wimmer, M.A., Jacobs, J.J., Fischer, A., Marks, L.D.: Graphitic tribological layers in metal-on-metal hip

- replacements. *Science* **334**(6063), 1687–1690 (2011). doi:[10.1126/science.1213902](https://doi.org/10.1126/science.1213902)
58. Buscher, R., Tager, G., Dudzinski, W., Gleising, B., Wimmer, M.A., Fischer, A.: Subsurface microstructure of metal-on-metal hip joints and its relationship to wear particle generation. *J. Biomed. Mater. Res. B Appl. Biomater.* **72**(1), 206–214 (2005). doi:[10.1002/jbm.b.30132](https://doi.org/10.1002/jbm.b.30132)
  59. Wimmer, M.A., Sprecher, C., Hauert, R., Tager, G., Fischer, A.: Tribochemical reaction on metal-on-metal hip joint bearings—a comparison between in vitro and in vivo results. *Wear* **255**(7–12), 1007–1014 (2003). doi:[10.1016/S0043-1648\(03\)00127-3](https://doi.org/10.1016/S0043-1648(03)00127-3)
  60. Zahiri, C.A., Schmalzried, T.P., Ebramzadeh, E., Szuszczewicz, E.S., Salib, D., Kim, C., Amstutz, H.C.: Lessons learned from loosening of the McKee-Farrar metal-on-metal total hip replacement. *J. Arthroplasty* **14**(3), 326–332 (1999). doi:[10.1016/S0883-5403\(99\)90059-1](https://doi.org/10.1016/S0883-5403(99)90059-1)
  61. Tager, K.H.: Studies on surface and new joint capsule of McKee-Farrar prosthesis implanted for several years. *Arch. Orthop. Trauma Surg.* **86**(1), 101–113 (1976). doi:[10.1007/Bf00415308](https://doi.org/10.1007/Bf00415308)
  62. Walker, P.S., Salvati, E., Hotzler, R.K.: The wear on removed McKee-Farrar total hip prostheses. *J. Bone Jt. Surg. Am.* **56**(1), 92–100 (1974)
  63. Mavraki, A., Cann, P.M.: Lubricating film thickness measurements with bovine serum. *Tribol. Int.* **44**(5), 550–556 (2011). doi:[10.1016/j.triboint.2010.07.008](https://doi.org/10.1016/j.triboint.2010.07.008)
  64. Mishina, H., Kojima, M.: Changes in human serum albumin on arthroplasty frictional surfaces. *Wear* **265**(5–6), 655–663 (2008). doi:[10.1016/j.wear.2007.12.006](https://doi.org/10.1016/j.wear.2007.12.006)
  65. Wang, A., Yue, S., Bobyn, J.D., Chan, F.W., Medley, J.B.: Surface characterization of metal-on-metal hip implants tested in a hip simulator. *Wear* **225**, 708–715 (1999). doi:[10.1016/S0043-1648\(98\)00384-6](https://doi.org/10.1016/S0043-1648(98)00384-6)
  66. Hesketh, J., Ward, M., Dowson, D., Neville, A.: The composition of tribofilms produced on metal-on-metal hip bearings. *Biomaterials* **35**(7), 2113–2119 (2014). doi:[10.1016/j.biomaterials.2013.11.065](https://doi.org/10.1016/j.biomaterials.2013.11.065)
  67. Myant, C., Cann, P.: In contact observation of model synovial fluid lubricating mechanisms. *Tribol. Int.* **63**, 97–104 (2013). doi:[10.1016/j.triboint.2012.64.029](https://doi.org/10.1016/j.triboint.2012.64.029)
  68. Wimmer, M., Mathew, M., Laurent, M., Nagelli, C., Liao, Y., Marks, L., Pourzal, R., Fischer, A., Jacobs, J.: Tribochemical reactions in metal-on-metal hip joints influence wear and corrosion. In: *Metal-On-Metal Total Hip Replacement Devices*. ASTM International (2013)
  69. Dugger, M.T.: Tribological Challenges in MEMS and Their Mitigation Via Vapor Phase Lubrication. In: George, T., Islam, M.S., Dutta, A.K. (eds.) *Proceedings of SPIE Micro- and Nanotechnology Sensors, Systems, and Applications Iii*, vol. 8031 (2011)
  70. Strawhecker, K., Asay, D., McKinney, J., Kim, S.: Reduction of adhesion and friction of silicon oxide surface in the presence of n-propanol vapor in the gas phase. *Tribol. Lett.* **19**(1), 17–21 (2005)
  71. Asay, D.B., Dugger, M.T., Kim, S.H.: In-situ vapor-phase lubrication of MEMS. *Tribol. Lett.* **29**(1), 67–74 (2007). doi:[10.1007/s11249-007-9283-0](https://doi.org/10.1007/s11249-007-9283-0)
  72. Asay, D.B., Kim, S.H.: Molar volume and adsorption isotherm dependence of capillary forces in nanoasperity contacts. *Langmuir* **23**(24), 12174–12178 (2007). doi:[10.1021/la701954k](https://doi.org/10.1021/la701954k)
  73. Carroll, B., Gogotsi, Y., Kovalchenko, A., Erdemir, A., McNallan, M.J.: Effect of humidity on the tribological properties of carbide-derived carbon (CDC) films on silicon carbide. *Tribol. Lett.* **15**(1), 51–55 (2003). doi:[10.1023/A:1023508006745](https://doi.org/10.1023/A:1023508006745)
  74. Ersoy, D.A., McNallan, M.J., Gogotsi, Y., Erdemir, A.: Tribological properties of carbon coatings produced by high temperature chlorination of silicon carbide. *Tribol. Trans.* **43**(4), 809–815 (2000). doi:[10.1080/10402000008982412](https://doi.org/10.1080/10402000008982412)
  75. Graham, E., Klaus, E.: Lubrication from the vapor phase at high temperatures. *ASLE Trans.* **29**(2), 229–234 (1986)
  76. Hook, D.A., Timpe, S.J., Dugger, M.T., Krim, J.: Tribological degradation of fluorocarbon coated silicon microdevice surfaces in normal and sliding contact. *J. Appl. Phys.* **104**(3), 034303 (2008)
  77. Tanner, D.M., Miller, W.M., Eaton, W.P., Irwin, L.W., Peterson, K.A., Dugger, M.T., Senft, D.C., Smith, N.F., Tangyunyong, P., Miller, S.L.: The effect of frequency on the lifetime of a surface micromachined microengine driving a load. In: *Reliability Physics Symposium Proceedings*. 36th Annual. 1998 IEEE International, pp. 26–35 (1998)
  78. Sung, D., Gellman, A.: The surface chemistry of alkyl and arylphosphate vapor phase lubricants on Fe foil. *Tribol. Int.* **35**(9), 579–590 (2002)
  79. Singer, I., Mogne, T.L., Donnet, C., Martin, J.: Friction behavior and wear analysis of SiC sliding against Mo in SO<sub>2</sub>, O<sub>2</sub> and H<sub>2</sub>S at gas pressures between 4 and 40 Pa. *Tribol. Trans.* **39**(4), 950–956 (1996)
  80. Hibi, Y., Enomoto, Y., Tanaka, A.: Lubricity of metal ethoxide formed on sliding surfaces of Si<sub>3</sub>N<sub>4</sub>-TiN-Ti composites in ethanol. *J. Mater. Sci. Lett.* **19**(20), 1809–1812 (2000). doi:[10.1023/A:1006742323483](https://doi.org/10.1023/A:1006742323483)
  81. Barnick, N.J., Blanchet, T.A., Sawyer, W.G., Gardner, J.E.: High temperature lubrication of various ceramics and metal alloys via directed hydrocarbon feed gases. *Wear* **214**(1), 131–138 (1998)
  82. Dugger, M.: *Nano/Micro-Tribology of MEMS*. In: vol. SAND2014-4771C. U.S. Department of Energy (2014)
  83. Asay, D.B., Dugger, M.T., Ohlhausen, J.A., Kim, S.H.: Macro-to nanoscale wear prevention via molecular adsorption. *Langmuir* **24**(1), 155–159 (2008). doi:[10.1021/la702598g](https://doi.org/10.1021/la702598g)
  84. Barbier, J.: Deactivation of reforming catalysts by coking—a Review. *Appl. Catal.* **23**(2), 225–243 (1986). doi:[10.1016/S0166-9834\(00\)81294-4](https://doi.org/10.1016/S0166-9834(00)81294-4)
  85. Forzatti, P., Lietti, L.: Catalyst deactivation. *Catal. Today* **52**(2–3), 165–181 (1999). doi:[10.1016/S0920-5861\(99\)00074-7](https://doi.org/10.1016/S0920-5861(99)00074-7)
  86. Trimm, D.L.: Control of coking. *Chem. Eng. Process.* **18**(3), 137–148 (1984). doi:[10.1016/0255-2701\(84\)80003-3](https://doi.org/10.1016/0255-2701(84)80003-3)
  87. Trimm, D.L.: Coke formation and minimisation during steam reforming reactions. *Catal. Today* **37**(3), 233–238 (1997). doi:[10.1016/S0920-5861\(97\)00014-x](https://doi.org/10.1016/S0920-5861(97)00014-x)
  88. Li, C., Stair, P.C.: Ultraviolet Raman spectroscopy characterization of coke formation in zeolites. *Catal. Today* **33**(1–3), 353–360 (1997). doi:[10.1016/S0920-5861\(96\)00120-4](https://doi.org/10.1016/S0920-5861(96)00120-4)
  89. Rostrup-Nielsen, J., Tottrup, P.: *Symp. Science of Catal. Appl. Industry, FPDIL Sindri* (39), 379 (1979)
  90. Guisnet, M., Magnoux, P.: Coking and deactivation of zeolites—influence of the pore structure. *Appl. Catal.* **54**(1), 1–27 (1989). doi:[10.1016/S0166-9834\(00\)82350-7](https://doi.org/10.1016/S0166-9834(00)82350-7)
  91. Rostrup-Nielsen, J.R.: Industrial relevance of coking. *Catal. Today* **37**(3), 225–232 (1997). doi:[10.1016/S0920-5861\(97\)00016-3](https://doi.org/10.1016/S0920-5861(97)00016-3)
  92. Gallezot, P., Leclercq, C., Guisnet, M., Magnoux, P.: Coking, aging, and regeneration of zeolites: VII. Electron microscopy and EELS studies of external coke deposits on USHY, H-OFF, and H-ZSM-5 zeolites. *J. Catal.* **114**(1), 100–111 (1988)
  93. Corthals, S., Van Nederkassel, J., Geboers, J., De Winne, H., Van Noyen, J., Moens, B., Sels, B., Jacobs, P.: Influence of composition of MgAl<sub>2</sub>O<sub>4</sub> supported NiCeO<sub>2</sub>ZrO<sub>2</sub> catalysts on coke formation and catalyst stability for dry reforming of



- methane. *Catal. Today* **138**(1–2), 28–32 (2008). doi:[10.1016/j.cattod.2008.04.038](https://doi.org/10.1016/j.cattod.2008.04.038)
94. Behera, B., Ray, S.S., Singh, I.D.: NMR Studies of FCC Feeds, Catalysts and Coke. In: Ocelli, M.L. (ed.) *Fluid Catalytic Cracking Vii Materials: Methods and Process Innovations*, vol. 166. *Studies in Surface Science and Catalysis*, pp. 163–200 (2007)
  95. Liu, B.S., Jiang, L., Sun, H., Au, C.T.: XPS, XAES, and TG/DTA characterization of deposited carbon in methane dehydroaromatization over Ga-Mo/ZSM-5 catalyst. *Appl. Surf. Sci.* **253**(11), 5092–5100 (2007). doi:[10.1016/j.apsusc.2006.11.031](https://doi.org/10.1016/j.apsusc.2006.11.031)
  96. Hardiman, K.M., Cooper, C.G., Adesina, A.A., Lange, R.: Post-mortem characterization of coke-induced deactivated alumina-supported Co–Ni catalysts. *Chem. Eng. Sci.* **61**(8), 2565–2573 (2006). doi:[10.1016/j.ces.2005.11.021](https://doi.org/10.1016/j.ces.2005.11.021)
  97. Tiratsoo, E.N.: *Natural Gas*, vol. 1979. Gulf Pub Co, Houston (1979)
  98. Rostrup-Nielsen, J.R.: Aspects of CO<sub>2</sub>-reforming of methane. In: Curry-Hyde, H.E., Howe, R.F. (eds.) *Studies in Surface Science and Catalysis*, vol. 81, pp. 25–41. Elsevier, Amsterdam (1994)
  99. Mizoh, Y.: Wear of tribo-elements of video tape recorders. *Wear* **200**(1–2), 252–264 (1996). doi:[10.1016/S0043-1648\(96\)07278-X](https://doi.org/10.1016/S0043-1648(96)07278-X)
  100. Bharat, B., Hahn, F.W.: Stains on magnetic tape heads. *Wear* **184**(2), 193–202 (1995)
  101. Rabinowicz, E.: The tribology of magnetic recording systems—an overview. *Tribol. Mech. Magn. Storage Syst.* **3**, 1–7 (1986)
  102. Mizoh, Y.: Wear of magnetic video head. *J. Jpn. Soc. Tribol.* **40**(12), 981–986 (1995)
  103. Osaki, H.: Flexible media—recent developments from the tribology point of view. *Tribol. Int.* **33**(5–6), 373–382 (2000). doi:[10.1016/S0301-679x\(00\)00057-8](https://doi.org/10.1016/S0301-679x(00)00057-8)
  104. Kuroe, A., Shinoda, F., Mikoda, M.: An experimental analysis of the recorded signal decrease phenomena in the repeated tape running. *Electr. Inf. Soc.* 194–200 (1991)
  105. Montgomery, R.S.: Run-in and glaze formation on gray cast iron surfaces. *Wear* **14**(2), 99 (1969). doi:[10.1016/0043-1648\(69\)90340-8](https://doi.org/10.1016/0043-1648(69)90340-8)
  106. Sugishita, J., Fujiyoshi, S.: The effect of cast iron graphites on friction and wear performance I: graphite film formation on grey cast iron surfaces. *Wear* **66**(2), 209–221 (1981)
  107. Takeuchi, E.: The mechanisms of wear of cast iron in dry sliding. *Wear* **11**(3), 201–212 (1968). doi:[10.1016/0043-1648\(68\)90558-9](https://doi.org/10.1016/0043-1648(68)90558-9)
  108. Leach, P.W., Borland, D.W.: The unlubricated wear of flake graphite cast-iron. *Wear* **85**(2), 257–266 (1983). doi:[10.1016/0043-1648\(83\)90068-6](https://doi.org/10.1016/0043-1648(83)90068-6)
  109. Erdemir, A.: Review of engineered tribological interfaces for improved boundary lubrication. *Tribol. Int.* **38**(3), 249–256 (2005). doi:[10.1016/j.triboint.2004.08.008](https://doi.org/10.1016/j.triboint.2004.08.008)
  110. Erdemir, A., Eryilmaz, O.L., Urgan, M., Kazmanli, K.: Method to produce catalytically active nanocomposite coatings. In: Google Patents (2013)
  111. Dowson, D., Jin, Z.M.: Metal-on-metal hip joint tribology. *Proc. Inst. Mech. Eng. H* **220**(2), 107–118 (2006). doi:[10.1243/095441105x69114](https://doi.org/10.1243/095441105x69114)
  112. Rostrup-Nielsen, J.R.: Sulfur-passivated nickel catalysts for carbon-free steam reforming of methane. *J. Catal.* **85**(1), 31–43 (1984). doi:[10.1016/0021-9517\(84\)90107-6](https://doi.org/10.1016/0021-9517(84)90107-6)
  113. Fang, S., Lin, G.X.: Managing varnish of turbine oil. In: Kim, Y.H., Yarlagadda, P. (eds.) *Materials, Mechanical and Manufacturing Engineering*, vol. 842. *Advanced Materials Research*, pp. 341–344 (2014)
  114. Bell, J., Tipper, J.L., Ingham, E., Stone, M.H., Fisher, J.: The influence of phospholipid concentration in protein-containing lubricants on the wear of ultra-high molecular weight polyethylene in artificial hip joints. *Proc. Inst. Mech. Eng. Part H-J. Eng. Med.* **215**(H2), 259–263 (2001). doi:[10.1243/0954411011533661](https://doi.org/10.1243/0954411011533661)
  115. Keenan, M.R., Kotula, P.G.: Accounting for poisson noise in the multivariate analysis of ToF-SIMS spectrum images. *Surf. Interface Anal.* **36**(3), 203–212 (2004)
  116. Tang, S., Gao, S., Hu, S., Wang, J., Zhu, Q., Chen, Y., Li, X.: Inhibition Effect of APCVD titanium nitride coating on coke growth during *n*-hexane thermal cracking under supercritical conditions. *Ind. Eng. Chem. Res.* **53**(13), 5432–5442 (2014). doi:[10.1021/ie401889p](https://doi.org/10.1021/ie401889p)
  117. Hibi, Y., Enomoto, Y.: Mechanochemical reaction and relationship to tribological response of silicon nitride in *n*-alcohol. *Wear* **231**(2), 185–194 (1999). doi:[10.1016/S0043-1648\(99\)00094-0](https://doi.org/10.1016/S0043-1648(99)00094-0)
  118. Mccarty, J.G., Wise, H.: Hydrogenation of surface carbon on alumina-supported nickel. *J. Catal.* **57**(3), 406–416 (1979). doi:[10.1016/0021-9517\(79\)90007-1](https://doi.org/10.1016/0021-9517(79)90007-1)
  119. Dowden, D.A.: Crystal and ligand field models of solid catalysts. *Catal. Rev.* **5**(1), 1–32 (1972). doi:[10.1080/01614947208076863](https://doi.org/10.1080/01614947208076863)
  120. Yan, Y., Neville, A., Dowson, D., Hollway, F.: Biotribocorrosion of CoCrMo orthopaedic implant materials—assessing the formation and effect of the biofilm. *Tribol. Int.* **40**(10–12), 1728 (2007). doi:[10.1016/j.triboint.2007.02.019](https://doi.org/10.1016/j.triboint.2007.02.019)
  121. Yan, Y., Neville, A., Dowson, D., Williams, S., Fisher, J.: Tribofilm formation in biotribocorrosion – does it regulate ion release in metal-on-metal artificial hip joints? *Proc. Inst. Mech. Eng. Part J. Eng. Med.* **224**(9), 997–1006 (2010). doi:[10.1243/13506501jet762](https://doi.org/10.1243/13506501jet762)
  122. Nakayama, K.: Triboemission of charged-particles from various solids under boundary lubrication conditions. *Wear* **178**(1–2), 61–67 (1994). doi:[10.1016/0043-1648\(94\)90129-5](https://doi.org/10.1016/0043-1648(94)90129-5)
  123. Nevshupa, R.A., Nakayama, K.: Triboemission behavior of photons at dielectric/dielectric sliding: time dependence nature at 10<sup>[sup -4]</sup>–10<sup>[sup 4]</sup>s. *J. Appl. Phys.* **93**(11), 9321 (2003). doi:[10.1063/1.1570934](https://doi.org/10.1063/1.1570934)
  124. Nevshupa, R.A., Nakayama, K.: Effect of nanometer thin metal film on triboemission of negatively charged particles from dielectric solids. *Vacuum* **67**(3–4), 485–490 (2002). doi:[10.1016/S0042-207x\(02\)00234-8](https://doi.org/10.1016/S0042-207x(02)00234-8)
  125. Ferrante, J.: Exoelectron emission from a clean, annealed magnesium single crystal during oxygen adsorption. *ASLE Trans.* **20**(4), 328–332 (1977). doi:[10.1080/05698197708982851](https://doi.org/10.1080/05698197708982851)
  126. Warren, W.L., Lenahan, P.M.: Electron-nuclear double-resonance and electron-spin-resonance study of silicon dangling-bond centers in silicon nitride. *Phys. Rev. B* **42**(3), 1773–1780 (1990)
  127. Podgornik, B., Hren, D., Vižintin, J.: Low-friction behaviour of boundary-lubricated diamond-like carbon coatings containing tungsten. *Thin Solid Films* **476**(1), 92–100 (2005). doi:[10.1016/j.tsf.2004.09.028](https://doi.org/10.1016/j.tsf.2004.09.028)
  128. de Barros’Bouchet, M.I., Martin, J.M., Le-Mogne, T., Vacher, B.: Boundary lubrication mechanisms of carbon coatings by MoDTC and ZDDP additives. *Tribol. Int.* **38**(3), 257–264 (2005). doi:[10.1016/j.triboint.2004.08.009](https://doi.org/10.1016/j.triboint.2004.08.009)
  129. Nakayama, K.: Triboemission of electrons, ions, and photons from diamondlike carbon films and generation of tribomicroplasma. *Surf. Coat. Tech.* **188**, 599–604 (2004). doi:[10.1016/j.surfcoat.2004.07.103](https://doi.org/10.1016/j.surfcoat.2004.07.103)
  130. Sanchez-Lopez, J.C., Erdemir, A., Donnet, C., Rojas, T.C.: Friction-induced structural transformations of diamondlike carbon coatings under various atmospheres. *Surf. Coat. Tech.* **163**, 444–450 (2003). doi:[10.1016/S0257-8972\(02\)00641-2](https://doi.org/10.1016/S0257-8972(02)00641-2)
  131. Liu, Y., Erdemir, A., Meletis, E.I.: Influence of environmental parameters on the frictional behavior of DLC coatings. *Surf. Coat. Tech.* **94–5**(1–3), 463–468 (1997). doi:[10.1016/S0257-8972\(97\)00450-7](https://doi.org/10.1016/S0257-8972(97)00450-7)



132. Erdemir, A., Bindal, C., Fenske, G.R., Zuiker, C., Wilbur, P.: Characterization of transfer layers forming on surfaces sliding against diamond-like carbon. *Surf. Coat. Tech.* **86–7**(1–3), 692–697 (1996). doi:[10.1016/S0257-8972\(96\)03073-3](https://doi.org/10.1016/S0257-8972(96)03073-3)
133. Kim, D.S., Fischer, T.E., Gallois, B.: The effects of oxygen and humidity on friction and wear of diamond-like carbon-films. *Surf. Coat. Tech.* **49**(1–3), 537–542 (1991). doi:[10.1016/0257-8972\(91\)90113-B](https://doi.org/10.1016/0257-8972(91)90113-B)
134. Lhomme, V., Bruneau, C., Soyer, N., Brault, A.: Thermal behavior of some organic phosphates. *Ind. Eng. Chem. Prod. Res. Dev.* **23**(1), 98–102 (1984). doi:[10.1021/i300013a021](https://doi.org/10.1021/i300013a021)
135. Appleby, W.G., Gibson, J.W., Good, G.M.: Coke formation in catalytic cracking. *Ind. Eng. Chem. Process Des. Dev.* **1**(2), 102–110 (1962). doi:[10.1021/i260002a006](https://doi.org/10.1021/i260002a006)
136. Merkle, A., Erdemir, A., Eryilmaz, O., Johnson, J., Marks, L.: *In situ* TEM studies of tribo-induced bonding modifications in near-frictionless carbon films. *Carbon* **48**(3), 587–591 (2010)
137. Mangolini, F., Rose, F., Hilbert, J., Carpick, R.W.: Thermally induced evolution of hydrogenated amorphous carbon. *Appl. Phys. Lett.* (2013). doi:[10.1063/1.4826100](https://doi.org/10.1063/1.4826100)
138. Nalwa, H.S.: *Handbook of Surfaces and Interfaces of Materials*, Five-Volume Set. Elsevier Science, Amsterdam (2001)
139. Liao, Y., Marks, L.D.: Modeling of thermal-assisted dislocation friction. *Tribol. Lett.* **37**(2), 283–288 (2010). doi:[10.1007/s11249-009-9520-9](https://doi.org/10.1007/s11249-009-9520-9)